uOttawa

L'Université canadienne
Canada's university

FACULTÉ DES ÉTUDES SUPÉRIEURES ET POSTOCTORALES

uOttawa

L'Université canadienne
Canada's university

FACULTY OF GRADUATE AND POSDOCTORAL STUDIES

Anne-Marie Guédon
AUTEUR DE LA THÈSE / AUTHOR OF THESIS

M.Sc. (Geography)
GRADE / DEGREE

Faculty of Arts, Geography
FACULTÉ, ÉCOLE, DÉPARTEMENT / FACULTY, SCHOOL, DEPARTMENT

Characterization of Salinity and Sodicity in Semi-Arid Irrigated Agricultural Lands Using Remote Sensing

TITRE DE LA THÈSE / TITLE OF THESIS

A. Bannari
DIRECTEUR (DIRECTRICE) DE LA THÈSE / THESIS SUPERVISOR

CO-DIRECTEUR (CO-DIRECTRICE) DE LA THÈSE / THESIS CO-SUPERVISOR

EXAMINATEURS (EXAMINATRICES) DE LA THÈSE / THESIS EXAMINERS

M. Sawada

B. Lauriol

Gary W. Slater
Le Doyen de la Faculté des études supérieures et postdoctorales / Dean of the Faculty of Graduate and Postdoctoral Studies

Department of Geography
Faculty of Arts
University of Ottawa

Characterization of salinity and sodicity in semi-arid irrigated agricultural lands using remote sensing

Anne-Marie Guédon

Thesis submitted to the Faculty of Graduate and Postdoctoral Studies in partial fulfillment of the requirements for the Master of Science degree in Geography

Your file Votre référence
ISBN: 978-0-494-61289-7
Our file Notre référence
ISBN: 978-0-494-61289-7

Table of contents

List of figures

List of tables

ABSTRACT

Surface salinity processes are highly dynamic and the methods needed to properly detect them must respond to that dynamism making remote sensing a tool particularly well-suited for the management of salinized lands. It allows the monitoring of affected lands for the prevention of serious degradation through appropriate and timely action. It is less costly in terms of time and resources than conventional methods and it is suited to the monitoring of large areas. Researchers are exploring how it can be adapted to the detection of moderate levels of salinity that could perhaps help to better prevent further degradation.

The main aim of this research is to assess for the first time the potential of the ALI sensor (Advanced Land Imager) on board the EO-1 satellite, with its rich infrared bands, for the identification and mapping of salinity and sodicity. Through the testing of different salinity indices found in the literature, semi-empirical predictive models were developed which could be suited to the characterization and mapping of sodic and saline soil conditions in semi-arid agricultural areas, using the Tadla's irrigated perimeter of Morocco as a test case. Predictive models were based on a second order regression analysis calculated between the E.C. of soils affected by salinity and sodicity, and different spectral salinity indices using spectroradiometric ground measurements. Emphasis was placed on detecting slight and moderate soil salinity and sodicity, which has been considered a challenge in the past. Semi-empirical models were derived from the data, and applied to an ALI image for analysis. Visual comparisons and statistical validation of these models using ground truth were undertaken in order to identify the best model for the mapping of salinity and sodicity in the Tadla's irrigated perimeter of Morocco.

The NDSI model does not give any results, the corresponding map being almost completely black. The model based on the SI-1 and the SI-ASTER confuses vegetation with high salinity soils, though the model does bring out areas of lower salinity. Both the R^2 of .67 for the SI-1 and .65 for the SI-ASTER further reinforce that these models have too much confusion to be used with accuracy. The SSSI-1 is visually more detailed than the SI-1 and SI-ASTER in that it give us more that three classes of salinity, and visually gives a more detailed picture of the ground, though these details do not correspond to the ground truth: there is confusion between the classes in the mid-levels of salinity; and the higher classes of salinity do not appear in areas that are shown by the validation map to contain higher levels of salinity. The statistical validation of this model reinforces what is seen on the image with an R^2 of only 0.68.

The model based on the SSSI-2 clearly gives the best results in comparison to the ground truth. Its derived map gives the closet overall visual approximation of the E.C. map, with a whole range of values. With a statistical validation of $R^2 = .97$ to the ground truth, it is by far the best performing of any of the other models, and the different classes are statistically well separated, which further reinforces the accuracy of the visual analysis.

ACKNOWLEDGMENTS

First and foremost I would like to extend my deepest gratitude to my supervisor, Abdou Bannari. I would not have been able to complete this work without his assistance and encouragement. He managed to keep his patience through all my life's ups and down. I would also like to thank the other members of my committee, Dr. Bernard Lauriol and Dr. Michael Sawada, for making this whole experience less scary, and the Department of Geography for staying patient and providing the teaching assistantships which, in addition to providing financial support, were also essential to my academic development.

I am most thankful for my colleague and best friend, Melanie Robin. Her encouragement, belief in me and tireless support made it possible to get through even the most stressful time. She was my rock. Melanie, Natasha Crane and Matt Mannela gave me an unbelievable sense of camaraderie, for which I am eternally grateful.

I would like to extend my gratitude to the ORMVAT for providing the analysis of the electrical conductivity and pH of the sampled soils and also for their logistic support and advice in undertaking the field work. I would also like to thank the NATO, AUF, Natural Sciences and Engineering Research Council (NSERC) for the financial support which allowed this research to go forward and allowed me to present preliminary results at the ISPMSR conference in Switzerland.

Finally, to my mother who read draft after draft of everything I wrote and was always available to take some of the load off my shoulders. She has supported my choices in my academic life since the beginning of my studies, and time and again reinforced my belief in myself, and my enthusiasm for research work.

ATTESTATION

My intellectual contribution to the research and writing of the articles presented in this thesis are as follows:

The first article (Bannari, A., Guedon, A.M., El-Harti, A., Cherkaoui, F.Z. and El-Ghmari, A. (2008) **Characterization of Slight and Moderate Saline and Sodic Soils in Irrigated Agricultural Land Using Simulated Data of ALI (EO-1) Sensor**. *Journal of Soil Science and Plant Analysis*, Vol. 39, p. 2795-2811.) is the result of preliminary data collection for my research. My work included participation in the field work, preliminary research and literature review as well as much of the data handling and organization. I did the manipulation of the spectral data and the indices in the ALI bands.

The second article (Guedon, A.M., Bannari, A., El-Harti, A. and El-Ghamari (2009) **Modeling and Mapping Saline and Sodic Soils in Irrigated Agricultural Land)** represents the bulk of my contribution. In terms of direct research I did the selection of soils used in the models, the derivation of the semi-empirical models, the application of the models to the image, the analysis of the image data and the statistical validation. The literature review was also predominantly the result of my effort as was the actual writing of the text of the article.

I. GENERAL INTRODUCTION

I.1 Context

It is estimated that approximately 38% of global arable land has been degraded by poor management practices in the last fifty years (Gardner, 1996). Irrigation agriculture, when improperly managed, is one of the leading causes of the degradation observed in the health and productivity of arable land, primarily through the processes of salinization and sodification (Postel, 1999). The consequences of salinity and sodicity in the soil for crops range from a reduction in productivity to complete sterility (Smedema, 1995). Irrigation agriculture is essential to the global food supply, with an even more pronounced dependence in arid and semi-arid regions where high evaporation rates and low precipitation make irrigating necessary for agricultural production. Well-developed management strategies for the conservation of arable land are all the more essential given that 45% of the earth's surface is considered arid or semi-arid, while home to 38% of the world's population (Hillel, 2000). In most of the countries affected by salinity and sodicity there is a lack of information on the exact nature and extent of the problem which can prevent appropriate measures for mitigation and increase the risk of permanent damage to the productivity of the soil (Al-Khaier, 2003). This is the situation currently being faced by irrigated regions in Morocco. Over the last three decades, Morocco has been struck with a drought which has increased dependence on groundwater for the irrigation of agricultural crops. The use of poor-quality groundwater combined with agricultural intensification has led to a rise in the levels of salinity and sodicity in the soils of the irrigated perimeter of the Tadla region in Morocco. In order to properly manage this accelerated risk of degradation, the use of remote sensing presents an interesting option for regular monitoring on the extent and nature of the salinity and sodicity present. This study marks the first attempt to test the potential of the ALI sensor (Advanced Land Imager) onboard the EO-1 satellite for the identification and mapping of slight and moderate levels of salinity, using the irrigated Tadla perimeter in Morocco as a study site.

I.2 Hypotheses

The two principal hypotheses on which this study is based are: 1) Ground-based spectral measurements are excellent for modeling salinity and sodicity and 2) the spectral richness of the ALI-EO-1 allows for a good discrimination of the salinity and sodicity, especially at low and moderate levels, in irrigated agricultural lands in semi-arid regions.

I.3 Objectives

This study aimed to research for the first time the potential of the ALI (Advanced Land Imaging) sensor aboard the Earth observing (EO-1) satellite for the identification and cartography of salinity and sodicity of irrigated agricultural land in a semi-arid environment.

The objectives are as follows:

1. Spectral characterization of different degrees of salinity and sodicity in the soils.
2. Laboratory analysis of the soil samples in order to identify the different levels of electrical conductivity (E.C.) and the levels of pH.
3. Analyse of the spectral behavior of soils affected by salinity and sodicity in the ALI spectral bands in light of the laboratory analysis.
4. Establishment of semi-empirical relationship between the E.C. and the spectral indices derived from the spectral measurements of the soil in order to determine which model gives the most precise cartography of salinity and sodicity.
5. The application of the relationships obtained during objective 4 on the ALI-EO-1 image and the validation of the results obtained in comparison to the ground truth.

I. 4. Structure

The data of this study includes soil samples collected from the study site, spectroradiometric measurements, laboratory analyses and image data acquired through the ALI EO-1 sensor. Following the introduction, the body of this thesis will consist of two articles, the first of which will describe the results of objectives l, 2, 3 and 4. It outlines the results obtained from the spectral analysis of the soils sampled in the study site in light of their levels of salinity and sodicity and describes the preliminary statistical results of different salinity indices using the ALI bands when applied to the spectral signatures of the soil samples.

The second article completes objective four and then addresses objective five. The semi-empirical models developed using the different salinity indices and the spectral data are then applied to the image data. Visual analysis and statistical validation are done to assess which of the semi-empirical models allowed for the most precise cartography of the salinity present in study site.

The articles are followed by a conclusion that provides a summation of the findings presented in the articles and offers recommendations to highlight areas that warrant further investigation.

Communications in Soil Science and Plant Analysis, 39: 2795–2811, 2008

ISSN 0010-3624 print/1532-2416 online
DOI: 10.1080/00103620802432717

Characterization of Slightly and Moderately Saline and Sodic Soils in Irrigated Agricultural Land using Simulated Data of Advanced Land Imaging (EO-1) Sensor

A. Bannari,[1] A. M. Guedon,[1] A. El-Harti,[2] F. Z. Cherkaoui,[3] and A. El-Ghmari[2]

[1]Remote Sensing and Geomatics of Environment Laboratory, Department of Geography, University of Ottawa, Ottawa, Ontario, Canada
[2]Laboratoire de Télédétection et des SIG, Faculté des Sciences et Techniques, Béni-Mella, Morocco
[3]Laboratoire de Télédétection et SIG, Office Régional de Mise en Valeur Agricole du Tadla (ORMVAT), Fkih-Ben-Salah, Morocco

Abstract: Around the world, especially in semi-arid regions, millions of hectares of irrigated agricultural land are abandoned each year because of the adverse effects of irrigation, mainly secondary salinity and sodicity. Accurate information about the extent, magnitude, and spatial distribution of salinity and sodicity will help create sustainable development of agricultural resources. In Morocco, south of the Mediterranean region, the growth of the vegetation and potential yield are limited by the joint influence of high temperatures and water deficit. Consequently, the overuse of surface and groundwater, coupled with agricultural intensification, generates secondary soils salinity and sodicity. This research focuses on the potential and limits of the advance land imaging (EO-1 ALI) sensor spectral bands for the discrimination of slight and moderate soil salinity and sodicity in the Tadla's irrigated agricultural perimeter, Morocco. To detect affected soils, empirical relationships (second-order regression analysis) were calculated between the electrical conductivity (EC) and different spectral salinity indices. To achieve our goal, spectroradiometric measurements (350 to 2500 nm),

Received 30 April 2007, Accepted 8 September 2007
Address correspondence to A. Bannari, Remote Sensing and Geomatics of Environment Laboratory, Department of Geography, University of Ottawa, Ottawa, Ontario K1N 6N5, Canada. E-mail: abannari@uottawa.ca

field observation, and laboratory analysis (EC of a solution extracted from a water-saturated soil), and soil reaction (pH) were used. The spectroradiometric data were acquired using the ASD (analytical spectral device) above 28 bare soil samples with various degrees of soil salinity and sodicity, as well as unaffected soils. All of the spectroradiometric data were resampled and convolved in the solar-reflective spectral bands of EO-1 ALI sensor. The results show that the SWIR region is a good indicator of and is more sensitive to different degrees of slight and moderate soil salinity and sodicity. In general, relatively high salinity soils show higher spectral signatures than do sodic soils and unaffected soils. Also, strongly sodic soils present higher spectral responses than moderately sodic soils. However, in spite of the improvement of EO-1 ALI spectral bands by comparison to Landsat-ETM+, this research shows the weakness of multispectral systems for the discrimination of slight and moderate soil salinity and sodicity. Although remote sensing offers good potential for mapping strongly saline soils (dry surface crust), slight and moderately saline and sodic soils are not easily identified, because the optical properties of the soil surfaces (color, brightness, roughness, etc.) could mask the salinity and sodicity effects. Consequently, their spatial distribution will probably be underestimated. According to the laboratory results, the proposed Soils Salinity and Sodicity Indices (SSSI) using EO-1 ALI 9 and 10 spectral bands offers the most significant correlation (52.91%) with the ground reference (EC). They could help to predict different spatial distribution classes of slight and moderate saline and sodic soils using EO-1 ALI imagery data.

Keywords: Electrical conductivity, EO-1 Advanced Land Imaging sensor, remote sensing, salinity, sodicity, spectral indices, spectroradiometric data

INTRODUCTION

The increased use of ground- and surface water coupled with the agricultural intensification in the Tadla's irrigated perimeter, Morocco, are the major causes of soil degradation through secondary soil salinity and sodicity. It is common that both saline and sodic conditions occur together. Sodicity represents the amount of exchangeable sodium (Na+) in water and in soil. Sodicity in soils has a strong influence on the soil structure. Dispersion occurs when the clay particles swell strongly and separate from each other on wetting. On drying, the soil becomes dense, cloddy, and without structure (Charters 1993; Ford et al. 1993; Sumner et al. 1998). Sodic soils have a pH $>$ 8.2 and a preponderance of carbonate and sodium by bicarbonate (Richards 1954).

Salinity refers to the amount of soluble salt in soil, such as sulfates (SO_4), carbonates (CO_3), and chlorides (Cl). Strongly saline soils often exhibit a whitish surface crust when dry. The solubility of calcium sulfate, also called gypsum ($CaSO_4$), is used as the standard for comparing salinity levels. Unlike sodicity, water movements influence salinity. It

occurs in areas where saline ground waters are very close to or at the ground surface and evaporation exceeds precipitation (Dehaan and Taylor 2002). In irrigated lands, salinity occurs when salts are concentrated in soils by the evaporation of freestanding irrigation water. The major causes are a combination of poor land management and crude irrigation practices. These practices cause changes in soil and vegetation cover and ultimately loss of vegetation and agricultural productivity. Soil salinity is measured by ground-based geophysics, measurements of soil electrical conductivity (EC) using soil pastes, and water extracts. Saline soils have EC $> 4\,\mathrm{dS\,m^{-1}}$ at 25 °C and pH < 8.2 (Richards 1954).

Knowing when, where, and how salinity and sodicity may occur is very important to the sustainable development of any irrigated production system (Al-Khaier 2003). Remedial actions require reliable information to help set priorities and to choose the type of action that is most appropriate in each situation (Metternicht and Zinck 2003). Ground-based electromagnetic measurements of soil EC are generally accepted as the most effective method for quantification of soil salinity (Norman et al. 1989; cited in Dehaan and Taylor 2002). Unfortunately, these methods are expensive, are time-consuming, and need considerable human resources for land surveying. Moreover, the dynamic nature of soil salinity and sodicity in space and time makes it more difficult to use conventional methods for comparisons over large areas (IDNP 2002). A major challenge of remote sensing, as a potential alternative technique, is to detect different levels of soil salinity and sodicity (Fraser and Joseph 1998; Taylor et al. 1994). In fact, a large variety of remote sensing techniques have been used for identifying and monitoring salt-affected zones, including aerial photos; spectroradiometric measurements; and multispectral, hyperspectral, passive, and active microwave images (Chaturvedi et al. 1983; Singh and Srivastav 1990; Hick and Russel 1990; Taylor et al. 1996; Metternicht 1998; Dehaan and Taylor 2002; Metternicht and Zinck 2003).

The objective of this research is to analyze, for the first time, the potential and limits of the Advance Land Imaging (EO-1 ALI) sensor spectral bands for the discrimination of slight and moderate secondary soil salinity and sodicity in the Tadla's irrigated agricultural perimeter, Morocco. Empirical relationships (second-order regression analysis) were calculated between the EC and different spectral salinity indices to detect slight or moderate soil salinity and sodicity. To achieve our goal, spectroradiometric measurements (350 and 2500 nm), field observations, and laboratory analysis [EC of a solution extracted from a water-saturated soil and soil reaction (pH)] were used. The spectroradiometric data were acquired during the summer season using the ASD (analytical spectral device) above 28 bare soil samples with various levels of salinity and sodicity, as well as unaffected soils. All of the spectroradiometric

data were resampled and convolved to match the solar-reflective spectral bands of the EO-1 ALI sensor using the updated Herman transfer radiative code, H5S (Teillet and Santer 1991).

MATERIALS AND METHOD

Study Site

The irrigated agricultural land of the Tadla region is one of the most important in Morocco. It is situated 30 km from the city of Béni-Mellal, at foot of the middle Atlas Mountains, and about 200 km southeast of Casablanca (32° 21′ N, 6° 21′ W; Figure 1). The primary crops are grains, legumes, and sugar beets. Covering an area of 3600 km^2 and being at an average altitude of 400 m, the Tadla plain is bordered to the north by the phosphate plateau, to the south by the middle Atlas Mountains of Béni-Mellal, and to the east by the Oum-El-Rbia River. The river divides the irrigated perimeter into two subperimeters with different hydrological and hydrogeologic characteristics: Béni-Amir and Béni-Moussa (Hammani et al. 2004; Bellouti et al. 2002). The subperimeter of Béni-Moussa has been irrigated since 1954 with good-quality water from Bin-El-Ouidane dam (0.3 $g\,l^{-1}$ of calcite, halite, and gypsum). Béni-Amir has been irrigated since 1938 by water from Oum-El-Rbia River, and shows a salinity level of 2 $g\,l^{-1}$ (mostly calcite and halite). Historically, the Tadla's

Figure 1. Study site, Tadla's irrigated agricultural perimeter (Béni-Mellal, Morocco). (Figure available in color online.)

irrigated perimeter has gone through two periods in the evolution of its water resources. The first period, from 1938 to 1980, was characterized by an abundance of surface water. The second period started in 1981 with a persistent drought that continues to the present day and is defined by a large water shortage (Hammani et al. 2004). Indeed, because of the impact of climate change (higher temperatures and water deficit), with its average annual rainfall under 350 mm and an average annual evapotranspiration of 1800 mm, the region has become semi-arid. It shows the characteristics of vulnerable Mediterranean landscapes with respect to the processes of soil impoverishment and environmental degradation. Consequently, recourse to underground water resources has become essential, even though the water qualities are poor. Increasing groundwater use causes soil salinity and sodicity to become more pronounced in important areas of the Tadla plain (Debbarh and Badraoui 2002).

Soils Sampling and Laboratory Analysis

Four different soil classes characterize the Tadla irrigated perimeter. The "iso-humiques" class contains medium-brown subtropical soils, saline and saline-sodic brown subtropical soils, and medium chestnut soils. This class is the most dominant in the perimeter, representing about 83% of soils. The class of "calci-magnesique" soils includes brown limestones (11%), and "rendziniforme" soils. The class of "ferralitiques" soils with iron sesquioxides and the hydromorph soil class are poorly evolved (Bellouti et al. 2002).

Soil data collection was carried out during the dry season, between 25 August and 5 September 2005, in the Tadla's irrigated agricultural perimeter. The soil sampling data consisted of 28 samples, which were selected on the basis of the spatial representativeness of the major soil types, and various degrees of salinity and sodicity (Figure 2; Table 1). The map of salinity in Tadla's irrigated agricultural perimeter (Figure 2) was used as a reference for the sampling data. This map was generated using ground-based EC measurements and geostatistical analysis in ArcGIS environment (ORMVAT 2004). Samples were taken from the soil upper layer (5 cm deep). Observations and remarks about each sample (color, brightness, texture, etc.) were noted. The location of each point was recorded with a global positioning system (GPS) unit and photographed using a 35-mm digital camera equipped with a 28-mm lens.

The laboratory analyses consisted of EC extracted from a soil with a water-saturated past and soil reaction (pH). These elements were analyzed in the laboratory using the current international standards methods in soil science (Baize 1988). Based on the results of our analyses, and according to Metternicht and Zinck (1997), we established three salinity classes using EC (nonsaline: 0 to 4 $dS\,m^{-1}$, slight: 4 to 8 $dS\,m^{-1}$, and moderate: 8 to

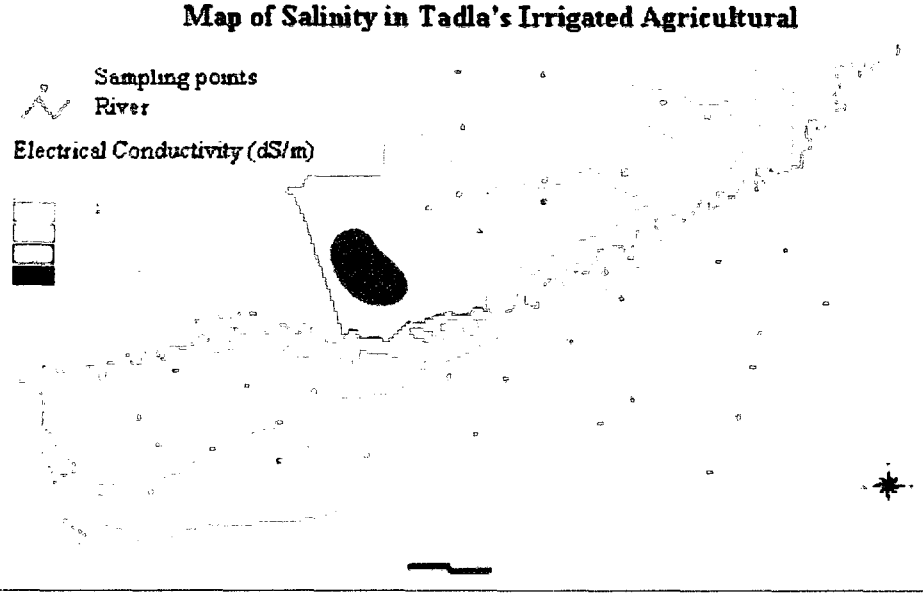

Figure 2. Map of salinity in Tadla's irrigated agricultural perimeter (Béni-Mellal, Morocco). Source: ORMVAT 2004. (Figure available in color online.)

16 dS m^{-1}), and three sodicity classes using pH (slight: 7 to 8 pH, moderate: 8 to 8.5 pH, and strong: 8.5 to 9 pH). Seven informational classes resulted from the combination of salinity and sodicity classes (Table 1).

Spectroradiometric Measurements

After the soil sampling and before the laboratory analysis, spectroradiometric measurements were acquired above the 28 bare soil samples using the ASD spectroradiometer (ASD Inc, 1999). This instrument is equipped with three detectors operating in the visible, NIR, and SWIR regions between 350 and 2500 nm. It allows a continuous spectral signature with 1.4-nm sampling step in the areas from 350 to 1000 nm and 2 nm in the areas of 1000 to 2500 nm. The system resamples the measurements with a 1-nm step, which allows the acquisition of 2151 contiguous bands per spectrum. The sensor is characterized by the programming capacity of the integration time, which allows an excellent performance of the signal-to-noise ratio, as well as a great stability.

Measurements were taken at the laboratory using two halogen lamps of 500 W each, equipped with an electrical current regulator. The data were acquired at nadir with a FOV (field of view) of 25° and an illumination angle approximately 5° from the vertical. The spectroradiometer was installed on a tripod at a height of approximately 30 cm from the target, which made it possible to observe a surface area of 177 cm^2. A laser beam

Table 1. Informational classes resulting from the combination of salinity and sodicity classes

Salinity and sodicity class	Soil no.	EC	pH
Moderate salinity and slight sodicity	4	8.28	8.0
	7	11.06	7.8
	9	11.19	8.2
	11	10.42	8.0
	18	9.68	8.0
Moderate salinity and moderate sodicity	17	14.58	8.1
Slight salinity and moderate sodicity	10	5.83	8.1
	21	6.17	8.0
Slight salinity and strong sodicity	16	5.87	8.5
	22	4.2	8.68
Nonsaline and slight sodicity	3	0.97	8.0
	5	0.85	8.0
	6	1.72	8.0
	8	3.33	7.8
	12	2.22	8.0
	14	1.76	8.0
	24	0.57	7.94
	25	1.88	7.7
	27	0.79	7.83
Nonsaline and moderate sodicity	1	1.8	8.2
	2	0.66	8.1
	13	2.94	8.4
	19	2.44	8.1
	23	0.69	8.21
	26	0.86	8.25
	28	1.45	8.01
Nonsaline and strong sodicity	15	0.77	8.51
	20	1.52	8.5

was used to locate the center of the ASD FOV compared to the center of each sample. The reflectance factor of each soil sample was calculated in accordance with the method described by Jackson et al. (1980) by rationing target radiance to the radiance obtained from a calibrated 25-cm by 25-cm white Spectralon panel (Labsphere 2001). Corrections were made for the wavelength dependence and non-Lambertien behavior of the panel. The Spectralon radiance was acquired immediately prior to the target radiance. The average of 25 spectra was convolved in the solar-reflective spectral bands of EO-1 ALI sensor using the updated Herman transfer radiative code, H5S (Teillet and Santer 1991).

Advanced Land Imaging Sensor

Launched in November 2000, the Advance Land Imaging (ALI) is the first Earth-observing (EO-1) sensor to be flown under NASA's New Millennium Program. This sensor was designed as a technology validation instrument for the next generation of Landsat-like instruments. It is a push-broom sensor that employs linear array technology, which is geometrically more stable than the cross-track scanning of MSS, TM, and ETM+ systems (Ungar 2001). This stability allows a simpler, less time-dependent geometric modeling approach but brings with it new challenges associated with the increased focal plane complexity (Storey, Choate, and Meyer 2004). Indeed, ALI employs novel wide-angle optics and highly integrated multispectral and panchromatic spectrometers. It uses a triplet telescope with visible, near infrared, and shortwave infrared focal planes. The instrument focal plane is partially populated with four sensor chip assemblies (SCA), and each covers 3° by 1.625° (NASA 2006). Each of the four SCAs contains 320 detectors (i.e., pixels) in the cross-track direction. For the panchromatic band, each SCA contains 960 detectors in the cross-track direction. There is an overlapping coverage of approximately 10 detectors between each adjacent pair of SCAs for the multispectral bands. For the panchromatic band, there is a coverage overlap of approximately 30 detectors between each adjacent pair of SCAs (NASA 2006). Operating at an orbit of 705 km, the EO-1 ALI across-track ground swath width is 37 km and the along-track length is normally 42 km. The pixel size is very similar to Landsat-7 ETM+, except for the higher-resolution (10 m) in the panchromatic (band 1) for ALI, and 30 m in all other bands, 2 to 10 (NASA 2006). Five bands mimic the ETM+ bands 1, 2, 3, 5, and 7. ETM+ band 4 is split into two bands covering 775–805 nm and 845–890 nm. In addition, there are two new additional bands labeled 2 and 8 at 433–453 nm and 1200–1300 nm, respectively, with 30-m pixel size (Bicknell et al. 1999). Table 2 presents the spectral bands of the EO-1 ALI sensor and their respective wavelengths, and Figure 3 shows the VNIR and SWIR normalized solar-reflective spectral response profile of ALI (EO-1) sensor.

Salinity Indices

In the literature, different spectral salinity indices are proposed for salt mineral detection and identification, at least when they are the dominant soil constituent. To retrieve information on the salt-affected areas from the LISS-II sensor of the IRS-1B satellite, Khan et al. (2001) proposed three spectral salinity indices: the brightness index (BI), normalized difference salinity index (NDSI), and salinity index (SI). Among these indices, they found that NDSI provided satisfactory results retrieving

Table 2. Spectral bands of EO-1 ALI sensor

Band	Wavelength (nm)
1[a]	480–690
2	433–453
3	450–515
4	525–605
5	630–690
6	775–805
7	845–890
8	1200–1300
9	1550–1750
10	2080–2350

[a]Panchromatic band.

different salt classes. According to Al-Khaier (2003), the ASTER salinity index (ASTER-SI), which uses bands 4 and 5, accurately detects overall salinity in bare agricultural soils. A methodology was proposed by the Indo-Dutch Network Project (IDNP 2002) for identification of soil salinity conditions using remote sensing Landsat-TM system and GIS. Amongst several remote sensing techniques, this project proposes three different salinity indices: SI-1, SI-2, and SI-3. The last is similar to the ASTER-SI index. In this research, all these indices were considered, calculated in EO-1 ALI spectral bands, and tested for the detection of slight and moderate soil salinity and sodicity effects.

$$\mathrm{BI} = \sqrt{ALI5^2 + ALI6^2} \tag{1}$$

$$\mathrm{NDSI} = \frac{(ALI5 + ALI7)}{(ALI5 + ALI7)} \tag{2}$$

$$\mathrm{SI} = \sqrt{ALI3 \times ALI5} \tag{3}$$

$$\mathrm{ASTER} - \mathrm{SI} = \frac{(ALI9 - ALI10)}{(ALI9 + ALI10)} \tag{4}$$

$$\mathrm{SI} - 1 = \frac{(ALI9)}{(ALI10)} \tag{5}$$

$$\mathrm{SI} - 2 = \frac{(ALI6 - ALI9)}{(ALI6 + ALI9)} \tag{6}$$

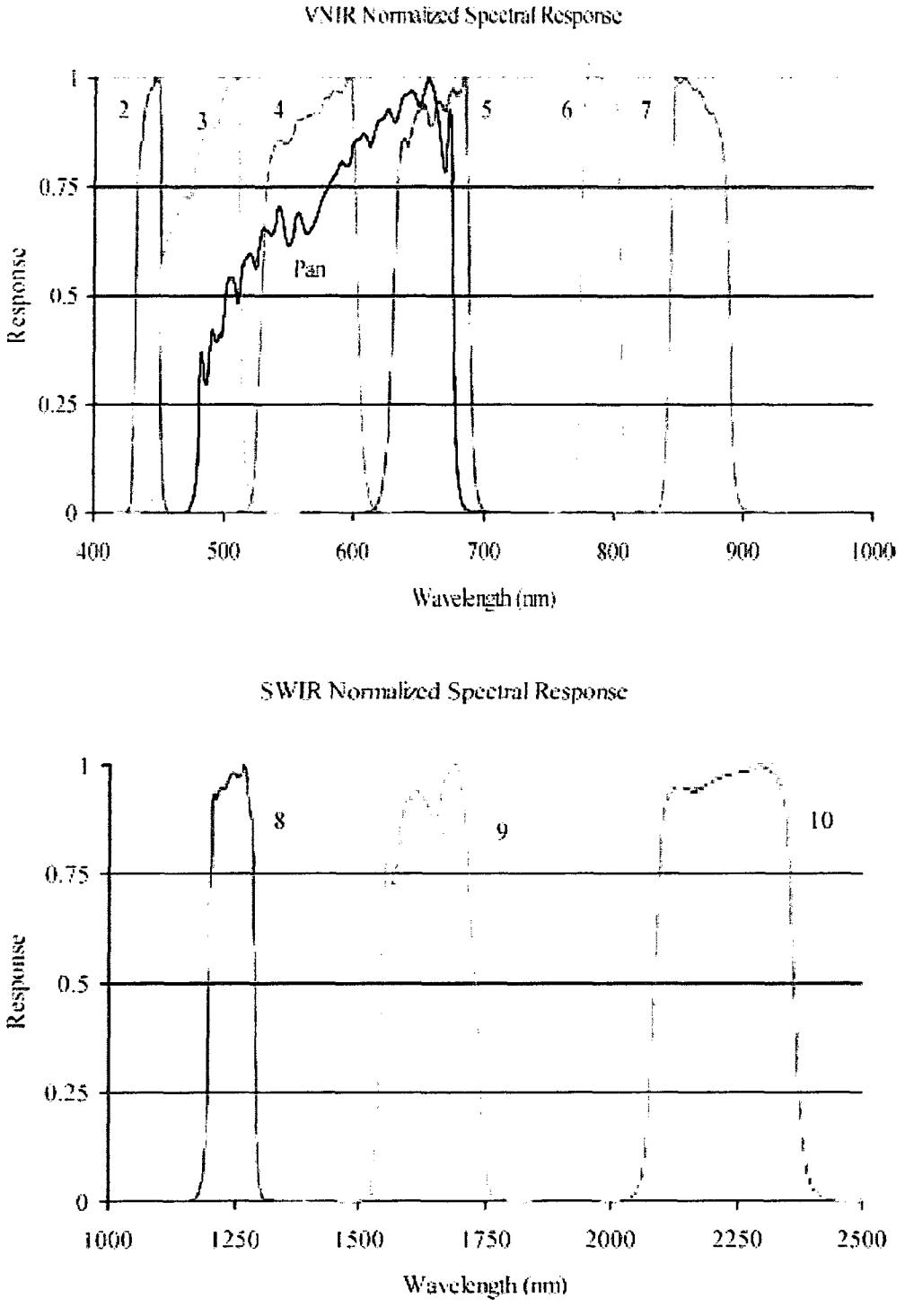

Figure 3. VNIR and SWIR normalized solar-reflective spectral response profile of ALI (EO-1) sensor. (Figure available in color online.)

$$\text{SI} - 3 = \frac{(ALI9 - ALI10)}{(ALI9 + ALI10)} \tag{7}$$

RESULTS AND DISCUSSION

Soil spectral signatures can provide information on the soil properties and quality. Indeed, there is a high correlation between soil reflectance and soil properties such as organic-matter content, moisture content, mineral composition, iron oxide content, color, brightness, roughness, size and shape of the soil aggregate, and the salt and sodium content. Figure 4 illustrates the spectral signature of the soils measured for this study. In general, this figure illustrates that moderately saline soils show higher spectral signature than do sodic and unaffected soils. Strongly sodic soils show higher spectral response than do moderately sodic soils. Unaffected soils, which have good structure and high organic matter, show very low spectra. Indeed, moderately saline soils are relatively smoother than soils with good structure and cause high reflectance in the visible and near infrared bands, especially when soil is dry. These observations are very clear when we resample the data in the EO-1 ALI sensor spectral bands and compare various degrees of soil salinity, sodicity, and vegetation cover (Figure 5). This figure also shows that the spectral properties of the soil salinity and sodicity are detectable in the visible and near infrared but are most evident in the SWIR region.

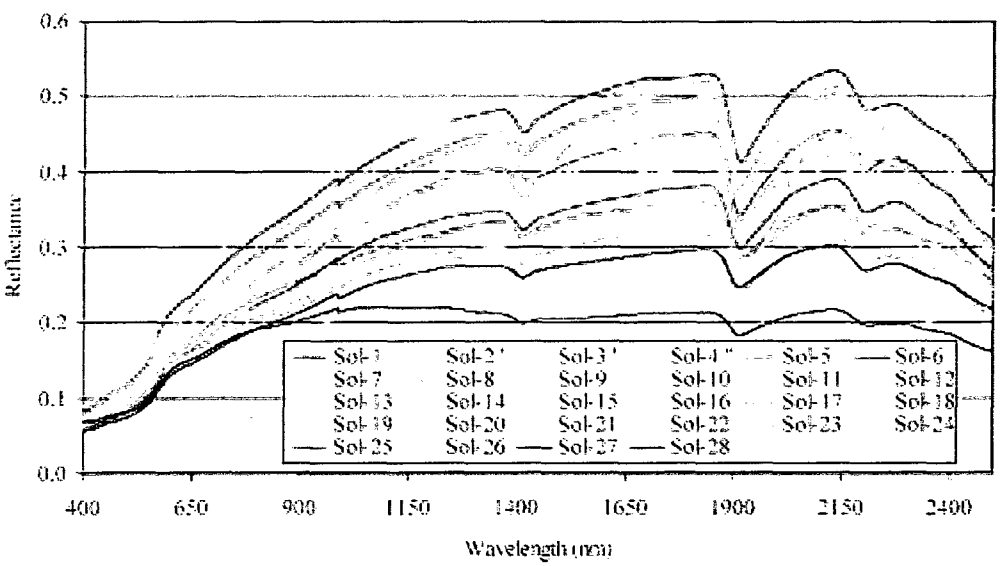

Figure 4. Spectral signatures of the considered soils. (Figure available in color online.)

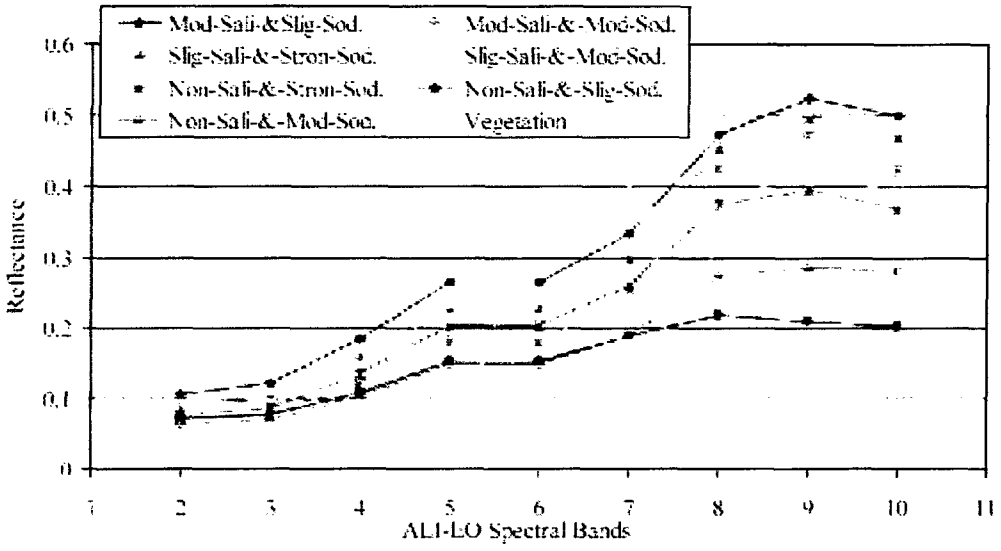

Figure 5. Resampled and convolved spectra in EO-1 ALI spectral bands for vegetation, unaffected soil, slightly and moderately saline soils, and sodic soil. (Figure available in color online.)

However, in spite of this capability, the color, brightness, and the roughness of the soil surfaces have a strong impact on the spectral signature (Figure 4). For instance, after irrigation, the fine soil surfaces become dry and smooth and change the optical properties. As well, the spatial distribution of particle size, the roughness, and the texture of the soil surfaces change. Consequently, the spectral signature of soil increases

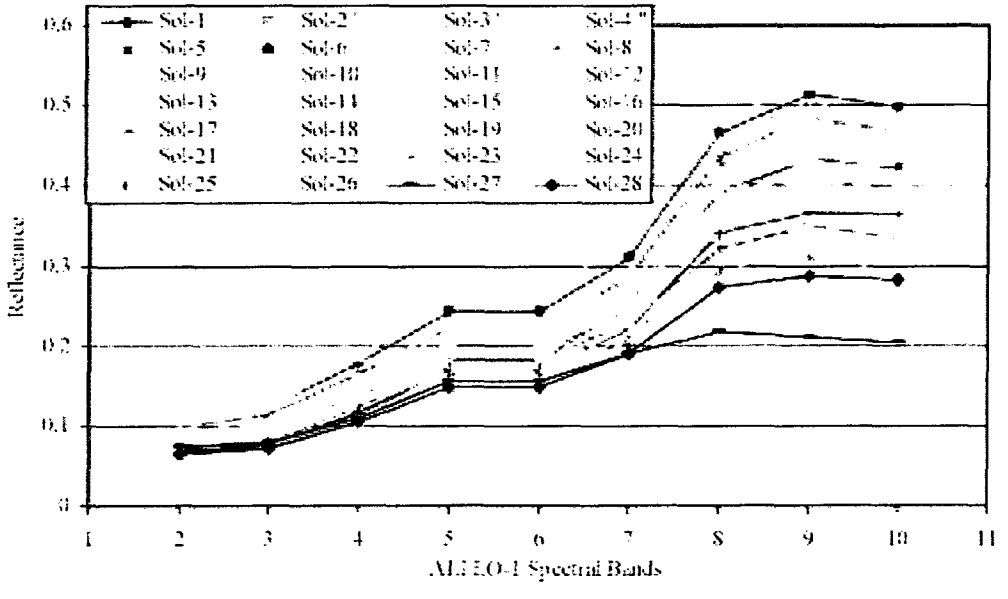

Figure 6. Resampled and convolved spectra in EO-1 ALI spectral bands. (Figure available in color online.)

automatically and masks moderate or slight salinity and sodicity effects (Figures 4 and 6). Even if the spectral reflectance in the near infrared and SWIR wavelengths provides a rapid and expressive means of characterizing strongly saline and sodic soils, it is probable that spectral confusion occurs between moderate or slightly saline and sodic soils, and unaffected soils with bright and clear color. For instance, soils 3 and 6 show the same level of salinity and sodicity, but their spectral signatures are different because of the difference of their optical proprieties (Figure 4 and Table 1). Although soil 6 is nonsaline with slight sodicity (good structure with organic matter), its signature is similar to that of soil 11, which is moderately saline. The spectral signature of soils 7 and 16 are alike but not their degrees of salinity and sodicity or their color. These observations are in agreement with other research using field or laboratory analysis or testing other satellite sensors (Chapman et al. 1989; Hick and Russel 1990; Crowley 1991; De Jong 1992; Mougenot et al. 1993; Rao et al. 1995; Metternicht and Zinck 1997; Goldshleger et al. 2001). Furthermore, even if the saline soil can be characterized by having different absorption features, Figure 2 shows that it is not possible to characterize, or to distinguish between, slight or moderate saline and sodic soils by their absorption features. This was not expected because the salt and sodium content status was not very strong in the soil samples and, consequently, these absorption features are absent.

To detect slight and/or moderate saline and sodic affected soils, empirical relationships (second-order regression analysis) were undertaken between the EC (ground reference) and different spectral salinity indices. Table 3 presents the resulting correlation coefficients at significance level $P < 0.001$. Among the indices proposed in the literature, only the ASTER-SI (similar to SI-3) provides the highest correlation (46.9%), especially when we consider just the saline and sodic soils. However, this correlation is not significant enough to retrieve very accurate information. Khan et al. (2001) found that NDSI provides satisfactory results, retrieving different salt classes (dry surface crust), but the research here shows that this index offers a very low correlation coefficient of 22.82% (especially when we consider all soils). If we take into account only the affected soils, this coefficient increases to 42.69%. The other indices show their limitation and a very low potential discrimination between slight and moderate soil salinity and sodicity effects, and unaffected soils.

Furthermore, when we correlate EC with the reflectances in each of the EO-1 ALI spectral bands, bands 9 and 10 provide the highest correlation. Using these two SWIR spectral bands, we devised soil salinity and sodicity indices (SSSI). The SSSI-1 uses a simple difference between spectral bands 9 and 10, whereas SSSI-2 uses a normalized difference ratio. These empirical relationships are more useful than

Table 3. Correlation coefficient between EC and spectral soil salinity indices at significance level $P < 0.001$

Salinity index	Correlation coefficient (%)	
	All soils	Only saline sodic soils
SI	4.53	5.65
BI	6.63	2.21
SI-1	18.86	46.70
SI-2	12.88	36.07
SI-3	18.59	46.90
ASTER-SI	18.6	46.90
NDSI	22.82	42.69
SSSI-1	34.00	52.00
SSSI-2	34.21	52.91

individual spectral bands or the other indices. They offer a correlation coefficient of 52.91% at significance level $P < 0.001$ with the EC using a second-order regression analysis. This correlation is not so high, but it's the most significant one compared to the other indices (Table 3). According to these laboratory results, we note that in spite of this correlation, which is at the acceptable limit, the SSSI-1 and SSSI-2 could enhance the slight and moderate saline and sodic zones, and differentiate them from unaffected soils using EO-1 ALI imagery data.

$$\text{SSSI} - 1 = (ALI9 - ALI10) \tag{8}$$

$$\text{SSSI} - 2 = \frac{(ALI9 \times ALI10 - ALI10 \times ALI10)}{ALI9} \tag{9}$$

CONCLUSIONS

This research focused on the potential and limits of the Advance Land Imaging (EO-1 ALI) sensor spectral bands for the discrimination of slight and moderate soil salinity and sodicity in the Tadla's irrigated agricultural perimeter, Morocco. The results show that the SWIR region is a good indicator, being more sensitive to different degrees of slight and moderate soil salinity and sodicity. In general, relatively high salinity soils show higher spectral signatures than do sodic soils and unaffected soils. Also, strongly sodic soils present higher spectral responses than moderately sodic soils. However, in spite of the improvement of EO-1 ALI sensor spectral band characteristics in comparison to Landsat-ETM+, this research shows the limitation of multispectral systems for

slight and moderate soil salinity and sodicity discrimination. Although remote sensing offers a good potential for mapping strongly saline soils (dry surface crust), slight and moderate saline and sodic soils are not easily identified, because the optical proprieties of the soil surfaces (color, brightness, roughness, etc.) could mask the salinity and sodicity effects. Consequently, their spatial distribution will probably be underestimated. To detect slight and moderate soil salinity and sodicity effects, the SSSI using ALI spectral bands 9 and 10 offer the most significant correlation (52.91%) with the ground reference (EC). Even if this correlation is not so high, they could help to predict different spatial distribution classes of slight and moderate saline and sodic soils using EO-1 ALI imagery data.

ACKNOWLEDGMENTS

The authors thank NATO, Agence Universitaire de la Francophonie (AUF), Natural Sciences and Engineering Research Council (NSERC), and the University of Ottawa for their financial support. We thank Mr. Hammou El-Khamar, head of the ORMVAT, for his support and for the laboratory analysis. We are grateful to the Faculty of Science and Technology (FST) of Béni-Mellal and Mr. M. Farhi and Mr. R. Amediaz from the Office Régional de Mise en Valeur Agricole du Tadla (ORMVAT) for their support and assistance in the field work.

REFERENCES

Al-Khaier, F. 2003. *Soil salinity detection using satellite remotes sensing*. Master's thesis, International institute for Geo-information Science and Earth Observation, Enschede, the Netherlands.

Analytical Spectral Devices, ASD Inc. 1999. Available at http://www.asdi.com/products-spectroradiometers.asp

Baize, D. 1988. *Guide des analyses courantes en pédologie: choix expression, presentation et interpretation*. Paris, France: INRA.

Bellouti, A., F. Cherkaoui, M. Benhida, A. Debbarh, B. Soudi, and M. Badraoui. 2002. Mise en place d'un système de suivi et de surveillance de la qualité des eaux souterraines et des sols dans le périmètre irrigué du Tadla au Maroc. In *Vers une maîtrise des impacts environnementaux de l'irrigation: Actes de l'atelier du PCSI*, ed. S. Marlet and P. Ruelle. Montpelier, France: CIRD.

Bicknell, W. E., C. J. Digenis, S. E. Forman, and D. E. Lencioni. 1999. EO-1 advanced land imager. *Proceedings of SPIE* 3750:80–88.

Chapman, J. E., D. A. Rothery, P. W. Francis, and A. Pontual. 1989. Remote sensing of vaporite mineral zonation in salt flats (salars). *International Journal of Remote Sensing* 10:245–255.

Chartres, C. J. 1993. Sodic soils: An introduction to their formation and distribution in Australia. *Australian Journal of Soil Research* 31:751–760.

Chaturvedi, L., K. Carver, J. Clifford Harlan, G. Hancock, F. Small, and K. Dalstead. 1983. Multispectral remote sensing of saline seeps. *IEEE Transactions on Geoscience and Remote Sensing* 21:231–239.

Crowley, J. K. 1991. Visible and near-infrared (0.4–2.5 μm) reflectance spectra of playa evaporite minerals. *Journal of Geophysical Research* 96 (16): 231–240.

Debbarh, A., and M. Badraoui. 2002. Irrigation et environnement au Maroc: Situation actuelle et perspectives. In *Vers une maîtrise des impacts environnementaux de l'irrigation: Actes de l'atelier du PCSI*, ed. S. Marlet and P. Ruelle. Montpelier, France. Available at http://doc.abhatoo.net.ma/doc/IMG/pdf/irrig.pdf

De Jong, S. 1992. The analysis of spectroscopical data to map soil types and soil crusts of Mediterranean eroded soils. *Soil Technology* 5:199–211.

Dehaan, R. L., and G. R. Taylor. 2002. Field-derived spectra of salinized soils and vegetation as indicators of irrigation-induced soil salinization. *International Journal of Remote Sensing* 80:406–417.

Ford, G. W., J. J. Martin, P. Rengasamy, S. C. Boucher, and A. Ellington. 1993. Soil sodicity in Victoria. *Australian Journal of Soil Research* 31:869–909.

Fraser, D., and S. Joseph. 1998. Mapping soil salinity in the Murray Valley (NSW) using satellite imagery. *Proceedings of the 9th Australasian Remote Sensing and Photogrammetry Conference*, vol. 1, paper no. 127, Sydney, Australia.

Goldshleger, N., E. Ben-Dor, Y. Benyamini, M. Agassi, and D. Blumber. 2001. Characterization of soil's structural crust by spectral reflectance in the SWIR region (1.2–2.5 μm). *Terra Nova* 13:12–17.

Hammani, A., M. Kuper, A. Debbarh, S. Bouarfa, M. Badraoui, and A. Bellouti. 2004. Evolution de l'exploitation des eaux souterraines dans le périmètre irrigué du Tadla. *Actes du séminaire sur la modernisation de l'agriculture irriguée* INCO-Wademed Seminar, 19–21 April 2004, Rabat, Morocco, 39–43. Rabat, Morocco: CIRD.

Hick, P. T., and W. G. R. Russel. 1990. Some spectral considerations for remote sensing of soil salinity. *Australian Journal of Soil Research* 28:417–431.

IDNP. 2002. *Indo-Dutch Network Project: A methodology for identification of waterlogging and soil salinity conditions using remote sensing*. Karnal, India: Central Soil Salinity Research Institute.

Jackson, R. D., P. J. Pinter, J. Paul, R. J. Reginato, J. Robert, and S. B. Idso. 1980. *Hand-held radiometry* (ARM-W-19). Phoenix, Ar.: U.S. Department of Agriculture Science and Education Administration.

Khan, N. M., V. V. Rastoskuev, E. V. Shalina, and Y. Sato. 2001. Mapping salt-affected soils using remote sensing indicators—A simple approach with the use of GIS IDRISI. In *Proceedings of the 22nd Asian Conference on Remote Sensing*. Singapore: Center for Remote Imaging, Sensing and Processing (CRISP), National University of Singapore; Singapore Institute of Surveyors and Valuers; Asian Association on Remote Sensing.

Labsphere. 2001. A guide to reflectance coatings and materials. Available at http://www.labsphere.com/tech_info/docs/Coating_&_Material_Guide.pdf.

Metternicht, G. I. 1998. Fuzzy classification of JERS-1 SAR data: An evaluation of its performance for soil salinity mapping. *Ecological Modelling* 111:61–74.

Metternicht, G. I. and J. A. Zinck. 2003. Remote sensing of soil salinity: Potentials and constraints. *Remote Sensing of the Environment* 85:1–20.

Metternicht, G. I., and J. A. Zinck. 1997. Spatial discrimination of salt- and sodium-affected soil surfaces. *International Journal of Remote Sensing* 18:2571–2586.

Mougenot, B. 1993. Effets des sels sur la réflectance et télédétection des sols salés. *Cahiers ORSTOM, Série Pédologie* 28:45–54.

NASA. 2006. *Earth Observing 1 (EO-1) user's guide.* Available at http://eo1.usgs.gov/userGuide/index. html.

Norman, C. P., C. W. Lyle, A. F. Heuperman, and D. Poulton. 1989. Tragowel Plains—Challenge of the plains. In *Tragowel Plains salinity management plan*, 49–89. Melbourne, Australia: Department of Agriculture.

ORMVAT. 2004. *Rapport sur le suivi de la qualité des sols.* Fkih-Ben-Salah, Morocco: Laboratoire de Télédétection et SIG, Office Régional de Mise en Valeur Agricole du Tadla (ORMVAT).

Rao, B., T. Sankar, R. Dwivedi, S. Thammappa, L. Venkataratnam, R. Sharma, and S. Das. 1995. Spectral behavior of salt-affected soils. *International Journal of Remote Sensing* 16:2125–2136.

Richards, L. A. 1954. *Diagnosis and improvements of saline and alkali soils* (U.S. Department of Agriculture Handbook 60). Washington, D.C.: U.S. Salinity Laboratory DA.

Singh, R. P., and S. K. Srivastav. 1990. Mapping of waterlogged and salt affected soils using microwave radiometers. *International Journal of Remote Sensing* 11:1879–1887.

Storey, J. C., M. J. Choate, and D. J. Meyer. 2004. A geometric performance assessment of the EO-1 Advanced Land Imager. *IEEE Transaction on Geosciences and Remote Sensing* 42 (3):602–607.

Sumner, M. E., W. P. Miller, R. S. Kookana, and P. Hazelton. 1998. Sodicity, dispersion, and environmental quality. In *Sodic soils—Distribution, properties, management, and environmental Consequences*, ed. M. E. Sumner and R. Naidu, 149–172. New York: Oxford University Press.

Taylor, G. R., A. H. Mah, F. A. Kruse, K. S. Kierein-Young, R. D. Hewson, and B. A. Bennett. 1996. Characterization of saline soils using airborne radar imagery. *Remote Sensing of Environment* 57:127–142.

Taylor, G. R., B. A. Bennett, A. H. Mah, and R. D. Hewson. 1994. Spectral properties of salinized land and implications for interpretation of 24 channel imaging spectrometry. In *Proceedings of the First International Remote Sensing Conference and Exhibition*, vol. 3, 504–513. Strasbourg, France: Taylor & Francis.

Teillet, P. M., and R. P. Santer. 1991. Terrain elevation and sensor altitude dependence in a semi-analytical atmospheric code. *Canadian Journal of Remote Sensing* 17 (1):36–44.

Ungar, S. G. 2001. Overview of EO-1: The first 120 days. *Proceedings of IGARSS* 1:43–45. Sydney, Australia: IGARSS.

Modeling and Mapping Slight and Moderate Saline and Sodic Soils in Irrigated Agricultural Land Using Remote Sensing

A.M. Guédon [1], A. Bannari [1], A. El-Harti [2], A. El-Ghmari [2]

[1] Remote Sensing and Geomatics of Environment Laboratory, Department of Geography, University of Ottawa, Ottawa (Ontario) K1N 6N5 Canada, Phone (613) 562-5800 (Ext. 1042), Fax (613) 562-5145, Email: abannari@uottawa.ca

[2] Laboratoire de Télédétection et des SIG, Faculté des Sciences et Techniques, Béni-Mella, Morocco

1. INTRODUCTION

1. 1 Purpose of the study

The irrigated perimeter of the Tadla in Morocco is only one instance among a multitude of locations where salinity and sodicity are fast becoming a serious problem. It is not a new phenomenon, but it is increasing in severity. Morocco has more than 148,000 ha of saline soils (Abrol *et al.*, 1988) and during the last three decades, a drought has impacted not only the regions that are dependent on rain-fed agriculture but also the irrigated perimeters. The reduction in the amount of water available for agricultural production because of decreased precipitation leads to an increase in the use of ground water. In the Tadla region in particular, agricultural intensification and the use of poor quality ground water are linked to rising levels of secondary soil salinity and sodicity.

This region has been selected to test, for the first time, the potential of the ALI sensor (Advanced Land Imager) on board the EO-1 satellite for the identification and mapping of salinity and sodicity in irrigated agricultural lands. Our hypothesis is that the spectroradiometric characteristics and the spectral richness of the ALI sensor would allow for better precision mapping of the levels of salinity and sodicity present in irrigated agricultural lands in semi-arid regions, and might even work for land characterized by

medium levels of salinity and sodicity as is the case in the Tadla perimeter. According to the literature, saline soils are easiest to differentiate using the infrared part of the spectrum (Bannari *et al.*, 2008). The ALI sensor on the EO-1 satellite has a greater number of infrared bands than any other multi-spectral sensor currently in orbit, and therefore presents a potential for a more precise identification of the presence and degree of salinization. Semi-empirical predictive models using a combination of ALI channels were tested to identify which one could offer the best tool for the identification of irrigation induced soil degradation.

1.2 Context of the study

Around the world cropland is often used as if it were an infinite resource, not taking into account the fact that opportunities to cultivate new land are dwindling and that permanent loss of cropland is an ever-increasing reality. Every year, precious arable land is lost to urban expansion and ongoing wear and tear on the soil (Gardner, 1996). It is estimated that 552 million hectares had been degraded by poor management practices since the Second World War, which represents approximately 38% of global arable land (Gardner, 1996). The process continues today with degradation severe enough to decrease productive land by 5 to 10 million hectares per year (Gardner, 1996).

Improperly managed irrigation agriculture is one of the leading causes of the degradation of the health and productivity of arable land. More precisely, the increasing use of both surface and ground water for irrigation can lead to soil degradation primarily through salinization and sodification (Postel, 1999). In appropriate quantities, dissolved mineral elements are essential to plant growth; however excessive quantities of dissolved salts affect plant development and cause a decrease in crop productivity. The salinization and sodification processes have consequences for crops, which range from reduction in productivity to complete sterility (Smedema, 1995).

Irrigated areas are estimated to account for 17% of the land currently in production in the world, and to contribute 30% of the total agricultural production; moreover, more than half of the recent increases in agricultural production globally come from the expansion of irrigated areas, which are now estimated to cover at least 270 million hectares (Smedema,

1995). Degradation to irrigated lands puts land essential to the global food supply at risk (Smedema, 1995).

The essential contribution of irrigation to the global food supply is even more important in semi-arid and arid regions where, by definition, water resources tend to be affected by high evaporation rates and low precipitation. 45% of the earth's surface is considered arid or semi-arid. 38% of the world population lives in these dry regions, and as demographic pressure increases, farming population begins to move into more and more marginalized areas already characterized by less productivity. In the marginalized areas in arid and semi-arid climates that tend to be less than ideal for food production, the addition of ground and underground water to precipitation is essential for effective agricultural production, and it allows farming in regions where it might otherwise be impossible (Hillel, 2000). Irrigation-based agriculture is therefore essential even as it brings with it the risk of soil degradation (Stewart, 2005).

Irrigation is particularly important in regions characterized the very climatic conditions that encourage the development of salinity and sodicity, that is, insufficient rainfall, and/or high evaporation, or conditions where the rainfall is poorly distributed during the year or is variable from year to year (Hillel, 2000). This is why salinization is a problem found predominantly in arid and semi-arid farming regions, such as those found in the agricultural regions of Morocco. Because the climatic conditions have such a strong influence on the occurrence of excess salinity, salinized soils have a distinct zonal pattern globally, with the affected areas being most widespread in areas where evaporation far exceeds rainfall. In such climates, leaching of salts out of the soil through rainfall is minimal and this leads to a general high level of salt concentration in the soil and in the water, both surface and groundwater (Smedema, 1995). As climate change impacts regions that are already affected by uncertain precipitation, irrigated areas become even more vulnerable.

Monitoring salinity and sodicity is vital to the health of irrigated agricultural areas since even lightly and moderately degraded lands yield less than they otherwise would. In addition, if the condition is left to persist and no mitigating measures are undertaken, the salinity and sodicity can become permanent and render the soil useless for growing crops, or at the very least decrease the productivity (Gupta and Abrol, 1990). The problem is compounded by the fact that in almost all countries affected by salinity there is a lack of

information on the exact nature and extent of the problem. Knowing when, where and how salinity and sodicity may occur is very important to the sustainable development of any irrigated production system (Al-Khaier, 2003).

1.3. Definition of salinity, its impact and its manifestation

Soils naturally contain salts in varying quantities; when these salts are mobilized they cause salinization by becoming concentrated in certain areas (Ghassemi *et al.*,1995). Because salinity is usually accompanied by sodicity, most researchers either use the terms salinity and salinization to denote both salinity and sodicity, or do not consider sodicity at all. Sodicity is only rarely considered in isolation.

Salinization has it sources in several processes that can work separately or cumulatively. Natural reserves of salts dissolved from the bedrock or already contained in the soil can be mobilized by water; and salts, once dissolved, are moved around by water into the affected zones, through a varied processes depending on the local geological and geographical characteristics. They tend to end up in the geohydrological sink areas where the water collects and/or stagnates (Smedema, 1995; Vincent *et al.*, 1995). Once the water is evaporated, the salts remain in place, in increasing concentrations. The progressive concentration of minerals is expressed in the rate of salinity and/or sodicity of the area. Where there is vegetation, underlying groundwater may also contribute salts to the root zone by capillary rise (Hillel, 2000), in addition, the roots of crop plants typically extract water from the soil while leaving most of the salts behind (Hillel, 2000; Verma *et al.*, 1994).

Soil salinity and soil sodicity are closely linked and commonly occur together in agricultural lands being irrigated by contaminated water. Salinity refers to the quantity in the soil of soluble salts such as sulphates (SO_4) Carbonates (CO_3) and chlorides (Cl). Sodic soils have a pH of more than 8.2 caused by the preponderance in carbonate and sodium bicarbonate (Richards, 1954). Sodicity represents the amount of exchangeable sodium (Na+) in water and in soil and has a strong influence on the soil structure. In wet sodic soils, dispersion occurs when the clay particles swell strongly and separate from each other. Upon drying, the soil becomes dense and cloddy and its structure, or lack of, prevents proper infiltration and aeration of the plants (Ghassemi *et al.*, 1995; Gupta and Abrol, 1990). The salinity-alkalinity of soil is discriminated into three classes by the US Salinity Laboratory (1954) mainly

saline, alkaline and saline-alkaline. Ranges of salinity and sodicity are usually described as slight, moderate or high based on the electrical conductivity and the percentage of exchangeable sodium or the sodium absorption ratio (Metternicht and Zinck, 1997). Soil salinity is customarily measured by assessing the soil electrical conductivity (E.C.) using the water extracted from a soil paste, which is considered by the literature to be the most accurate method to characterize soil salinity. A soil is said to be saline when it has an electrical conductivity of more than 4 ds/m at 25°C (Richards, 1954) though other factors such as mineral content (Peverill *et al.*, 1999) and soil characteristics (Friedman,2005) may affect the electrical conductivity, independent of salinity levels.

It is useful to distinguish between primary salinity, which is naturally occurring and is caused by the chemistry of the bedrock, and secondary salinity, which is brought about by human causes (Ghassemi *et al.,* 1995). Many natural factors influence the formation of salinization, including types and rate of rainfall, type of plant cover, (micro) topography, depth and nature of soil, and other incidental aspects of the location. Geological factors that affect the types of salt and the degree of severity present in a salinization situation include the geologic deposits, the acidity of the environment (and therefore the rate of dissolution of the salts), the chemistry of the surface and ground water deposited in or circulating through the affected environment (Jankowski and Ackworth, 1999). Secondary salinization finds its sources primarily in cultural factors usually involving farming methods leading to the reinforcing of natural processes. Among the most important causes of secondary salinization are certain types of soil management methods, especially the use of poorly adapted irrigation methods leading to high evaporation, bad drainage systems, and the use of saline irrigation waters or highly mineralized deep aquifers (Dehaan and Taylor, 2002; Badraoui *et al.,* 1998).

While primary salinity corresponds to processes that are relatively stable, secondary salinity can increase rapidly with intensifying human activities. Salinization most often occurs when salts are concentrated in the soil by the evaporation of water, either freestanding irrigation waters or ground waters that are very close to or at ground surface, so that high concentrations of salts often exhibit a whitish surface crust when they dry (Dehaan and Taylor, 2002). Many of the mineral elements contained in solution are a source of nutrition for plants; but an increase in the amount of salts dissolved in the water being taken by the

plant disturbs the osmotic pressure and leads to water stress in the crop. As the salinity levels in the root zones increases, the plant must spend more energy to take water from the same soil water content. High soil salinity can also cause nutrient imbalance and result in the accumulation of toxic elements in the plant (Al-Khaier, 2003).

1.4 Measuring, locating and monitoring saline soils using remote sensing

1.4.1 Requirements

Salinity and sodicity modify temporarily or permanently the state of the surface and of the soils below (Mougenot, 1993). For lands affected by salinization, there are methods available to slow down the processes and sometimes even reverse them. It is therefore possible to intervene. The introduction of suitable remedial irrigation practices can alleviate most of the problems, provided one knows how, when, and where salinity and sodicity are developing (Al-Khaier, 2003). Remedial actions require reliable information to help set priorities and to choose the type of action that is most appropriate in each situation (Metternicht and Zinck, 2003).

In affected areas, farmers, soil managers, scientists and agricultural engineers need accurate and reliable information on the nature, scope or extent, severity and spatial distribution of the salinity and sodicity against which they could take appropriate measures (Metternicht and Zinck, 2003). Without adequate information mitigation measures cannot be applied to the affected soils and damage becomes irreversible if left too long untreated. Soil salinity is highly dynamic and varies considerably in time and in space depending on many factors; so, in order to properly manage the situation, information must be not only accurate and reliable, but also up-to-date and on going. Because salinization, its effects, and whatever mitigation measures are taken, are all dynamic processes, they must be monitored regularly (Smedema, 1995).

1.4.2 Detecting salinity

Traditionally accepted to be the most effective way of measuring soil salinity, the ground-based measurement of the soil's E.C. using water extracted from a saturated paste gives very

good estimates of soil salinity. But the cost of conventional methods of mapping salinity based on such soil chemical analysis becomes prohibitive when they are associated with the regular monitoring necessary for saline soil management. These methods are financially expensive, time consuming, and need considerable human resources for land surveying, especially for large areas (IDNP, 2003). In addition, the dynamic nature of soil salinity and sodicity in space and time makes it very difficult to use conventional methods for comparisons over large areas (Norman *et al.,* 1989).

Various authors have examined the advantages of using remote sensing methods and sensors for the assessment of soil degradation due to sodicity and salinity (see among others Metternicht and Zinck, 1997; Dwivedi and Rao, 1992; Hashem *et al.*, 1997; Hicks and Russel, 1990; Goosens *et al.*, 1998; Mougenot *et al.,* 1993; Verma *et al.,* 1994; Zuluaga, 1990). Remote sensing observation methods are relatively easy to use and reliable in certain conditions. Their main advantage is that they allow the mapping of large areas at relatively low cost (Zinck, 2000; IDNP, 2002). Information can also be collected at regular intervals; monitoring becomes easier and less expensive which allows not only for the appropriate remedial action to be taken, but also for the monitoring of the effectiveness of any ongoing remediation or preventative measures, which facilitates management and decision-making (Zinck, 2000; IDNP, 2003).

The application of remote sensing using aerial photography for mapping salt-affected soils has been assessed (Rao *et al.,* 1991). But it is the advancements in multispectral, hyperspectral and radar technologies that are providing the best and newest opportunities for more precise and more effective mapping of soils. Multispectral remote sensing, in particular, can allow for relatively precise measurements of the saline conditions in a timely fashion especially for large areas. At the present time, remote sensing methods for the monitoring and mapping of salinity conditions in irrigated areas offer therefore very valuable tools to combat and control salinity in irrigated lands, since most countries affected by the problem cannot afford costly measures and the information gathering must be easy to use and low-cost (Smedema, 1995). But there are still difficulties in detecting the soil salinity and sodicity in certain conditions (Fraser and Joseph, 1998; Taylor *et al.,* 1994), especially in low and medium concentrations that are the most critical stages of soil degradation.

The wavelengths most commonly applied to land resources survey are those found between 0.4 and 1.5 nm (Al-Khaier, 2003); and salinity detection is no exception. Studies have been conducted in laboratory to determine the best spectral bands to detect saline and sodic soils and it is generally agreed that the SWIR is the most important for detection (Csillag *et al.*, 1993; Crowley, 1991). Hunt *et al.* (1971) and Drake (1995) have studdied the absorption bands of gypsum and other minerals which cause salinity and sodicity, identifying 1000, 1200, 1400, 1600, 1740, 1900 and 2200 nm as key regions for detection with small variations in absorptions between the different minerals. Mougenot *et al.*, (1993) and, later, Howari, (2002) analyzed the influence of spectral signature on the different types of saline crusts. Csillag *et al.* (1993) compared two types of soils to see the effect of sodicity and salinity on reflectance and Chapman *et al.* (1989) then Drake (1995) described the various absorption peaks of the salts found in agricultural regions. Mougenot *et al.* (1993) conducted studies with direct observations on bare soils and indirect observation on vegetation cover. This study and those conducted by Mulders (1987) and Rao *et al.* (1991) confirmed that bands found in the middle infrared were associated with information related to salt content differences and gave some information on salt types. Rao *et al.* (1991) also found that salt-affected soils, compared to normal cultivated soils, showed relatively higher spectral response in visible and near-infrared regions and strongly saline-sodic soils were found to have higher spectral response as compared to moderately saline-sodic soils.

Most sensors currently in orbit have spectral bandwidth in the visible and near-infrared and therefore can be useful to varying degrees depending on certain factors. However, the spectral bands found on most multispectral satellites tend to be large and can lack some of the sensitivity necessary to make a precise quantification of the amount of salt on the ground (Mougenot, 1993). Various authors including Mougenot (1993) and Casas (1995) have confirmed that while the remote sensing of very saline soils should presents very little difficulty, it can sometimes be very difficult to distinguish the varying degrees of salinity through remote sensing. Extreme levels of salinity concentrates salts on the bare soil surface where there often develops an efflorescent salt crust making salinity relatively easy to identify through remote sensing (Al-Khaier, 2003); but sodic soils and soils with slight salinity do not present obvious manifestations at the surface, and are therefore often poorly identified and under-estimated. Salinity cannot be detected in quantities of less that 10-15%

depending on the salts (Mougenot, 1993). Most authors are able to distinguish only 2 and 3 classes (strong and medium) of salinity levels with errors occurring in differentiating between moderately saline and normal soils (INDP, 2003). Metternicht and Zinck (1997) managed to obtain 64% discrimination between saline and non-saline soils, but they too concluded that spectral confusion could occur when one is trying to differentiate between different levels of salinity (Metternicht and Zinck, 2003).

The signal gathered by the sensor is affected by the different combinations of salt types, soil surface textures, and organic matter content; the main factors affecting the radiometric measurements in the visible and near-infrared wavelengths are the quantity and mineralogy of salts, the level of soil moisture, and the colour and roughness of the terrain (Metternicht and Zinck, 1997) and the vegetation. With so many factors influencing the signal received by the sensor, the search for and testing of tools to remedy spectral confusion when trying to identify saline and sodic soils has become important for many authors. Among them, Hashem *et al.* (1997) tackled the problem of salinity and sodicity detection in agricultural regions in Egypt by using a temporal comparison and images obtained from Landsat-TM and SPOT-HRRV. He reported that spectral confusion could occur between saline regions and desertified regions. Spectral confusion was also problematic for Verma *et al.* (1994) when he mapped salinity in certain regions of India using Landsat-TM and found that it was difficult to appreciate the difference between affected soils and fallow fields. Though the use of the thermal band will not be considered in this study, it should be noted that the use of thermal bands were shown to increase the precision of soil salinity estimates (Mougenot *et al.*, 1993); however the use of the thermal band alone gives poor results (Metternicht, 1996).

1.4.3 Hyperspectral Sensors

The possibilities presented by hyperspectral sensors for salinity detection have been investigated only recently. Taylor and Deehan (2000) used the Hymap airborne sensor and spectral unmixing. They found that the saline endmember presented a pronounced high reflectance at 800 nm and broad absorption features at 1450 and 1900 nm, and that subtle absorption features at 980 and 1170 nm can contribute to accurate mapping of salinity. Ben-Dor *et al.* (2002) obtained successful results with the DAIS-7915 hyperspectral sensor in the

visible and near infrared spectral bands, in producing maps not only of salinity but also of field soil moisture and organic matter.

Relatively few studies have been conducted on the detection of soil salinity using active remote sensing (radar and microwave), but they are considered potentially adequate for detecting salinity (Mettenicht and Zinck, 2003). Studies have focused on saline water detection (Singh and Srivastav, 1990) and discriminating salinity levels using ancillary data such as surface roughness and vegetation types in order to estimate the salinity (Metternicht, 1998; Taylor *et al.*, 1996). Mougenot *et al.* (1993) have noted that the characterisation of saline soils using an active signal such as radar requires some soil moisture to be effective. This can cause some difficulties when locating salt affected areas in arid landscapes where the amount of moisture is very low (Mettenicht and Zinck, 2003).

We can distinguish the direct effects of the presence of salt on the surface (crusts and saline efflorescence) not only through reflectance, but also by examining indirect effects on the type of vegetation and the stress of the plants (Zuluaga, 1990; Vidal *et al.,* 1996; Vincent et *al.,* 1995). Even the lack of vegetation all together can help detect extreme cases of salinity. There is an inverse relationship between reflectance and salinity, since salt content induces less plant cover. The consequences on vegetation of salinity can be seen by a decrease in the size of the plants and in their density, which corresponds to a similar increase in salinity in the soils and the groundwater (Mougenot, 1993).

Currently, the most heavily investigated method for salinity detection remains multispectral remote sensing with Landsat-TM being the sensor most in use (Mulder and Epma, 1986; Menenti *et al.*, 1991; Zuluaga 1990; Vincent *et al.,* 1995; Joshi *et al.,* 2002; Singh and Srivastav, 1990). ALI is a relative new comer in the field and has not been so far the object of many studies. Since it was launched in 2000 to test its potential to replace the Landsat series, few researchers have had the opportunity to study its performance, and even less to test its capacity in salinity detection.

1.5 Methodology of this study

For the purposes of this study, different soil samples taken from the Tadla's irrigated perimeter, representing varying levels of salinity and sodicity and considered representative of the soils present in the area, were collected. Their spectral characteristics were measured, and were then compared with and juxtaposed to the results of the chemical laboratory analysis in order to assess the impact of varying levels of salinity and sodicity on soil spectral behaviour (Bannari *et al.*, 2008). The observations made on the Tadla soils are in agreement with previous observations made in both laboratory analysis and the testing of other satellite sensors, which show that the presence of salinity and sodicity in the soil can increase the signal, particularly in the infrared bands (Chapman *et al.,* 1989; Hick and Russel, 1990; Rao *et al.*, 1991; Mougenot *et al.,* 1993; Rao *et al.,* 1995; Metternicht and Zinck, 1997).

The spectral information obtained from the Tadla soils was resampled and convolved into the ALI bands in order to get an estimate of how the study site soils would be detected with the ALI sensor. These bands were then used in the calculation of the different salinity indices. Each index was calculated using the corrected spectral bands in the EASI modeling function of PCI Geomatica.

Second order regressions were undertaken between the E.C. (ground reference) and different spectral salinity indices using Microsoft Excel. Other types of regressions were run, but second order regressions were found to perform better than the others. A second order regression was run using all of the published indices first with all affected and non affected soil, and then with a selection of only the affected soils. The resulting correlation coefficients were calculated at a 95% confidence interval, and semi-empirical predictive models were derived. The relationship was then plotted on a graph to see if the index could predict the level of salinity.

The model equations were applied to the ALI image and were visually analyzed for their potential in the detection and cartography of the different levels of salinity and sodicity in the study region, especially at low and moderate levels. The results were then compared with and validated through the ground truth map provided by the ORMVAT, both visually

and statistically. The methodology used is summarized in the organizing graph below in figure 1.

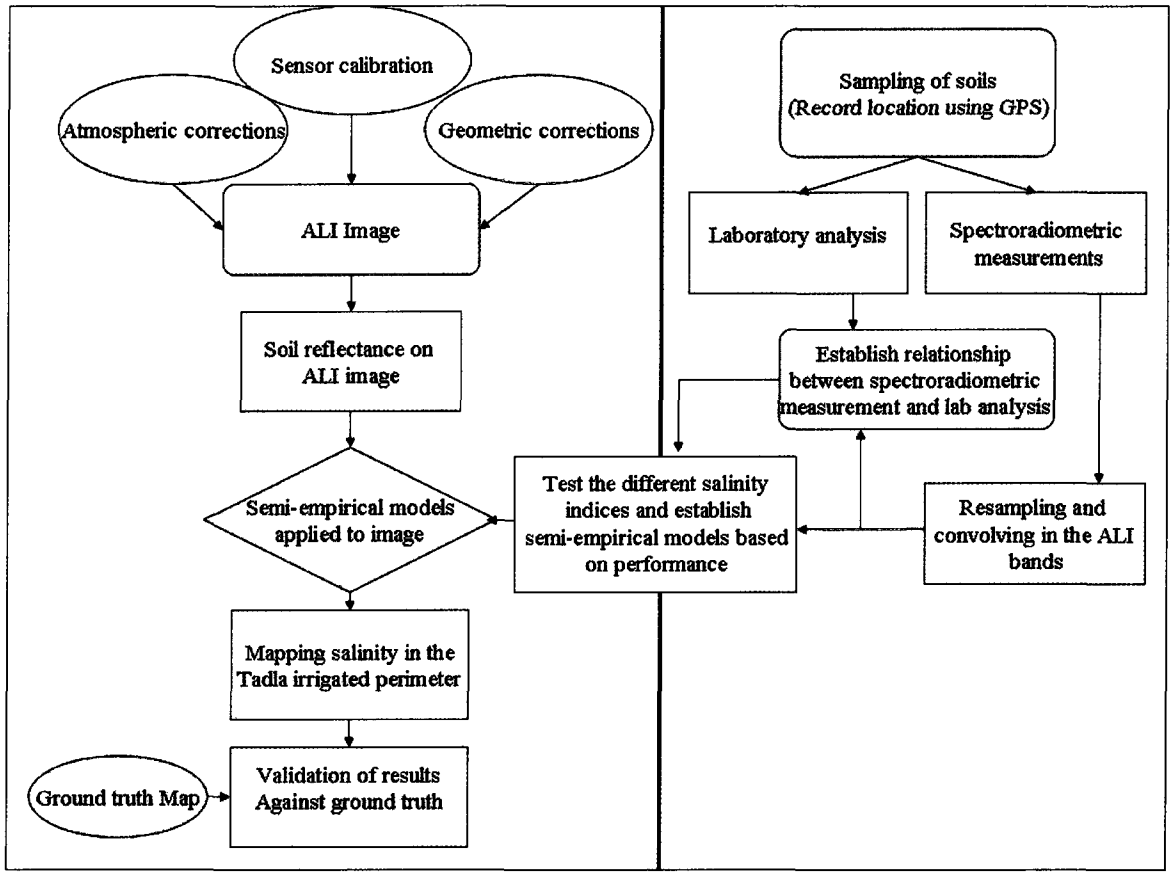

Figure 1: Methodology of study

2. MATERIALS AND METHODS

2.1 Study site

Morocco is situated on the North-West coast of the African continent, and though it covers about 71 million hectares, only 8.6 million of these can be used for agricultural production (FAO, 2005). About 78% of Moroccan land is considered desert or arid, and only 12% of the total land is considered arable, 1 200 000 hectares of which are irrigated. The Moroccan economy is primarily dependent on agricultural production, which is the primary source of

revenue and employment for 50% of the active population, as well as contributing 17% of the GDP (Berkat and Tazi, 2004).

The irrigated perimeter of the Tadla is one of the most important agricultural regions in Morocco. It is situated 30 km from the city of Beni-Mellal, at the foot of the middle Atlas mountains and is about 200 km from the city of Casablanca at 32° 21' N et 6° 21' W (Figure 2). The Tadla plain covers about 3600 km^2 and is located at an average elevation of 400 m. It is bordered on the North by phosphate plateaus, on the South by the Atlas mountains near Beni-Mellal, and to the East by the Oum-El-Rbia river. This river divides the irrigated perimeter into two sub-perimeters defined by different hydrologic and hydrogeologic characteristics: Béni-Amir and Béni-Moussa (Hammani *et al.*, 2004; Bellouti *et al.*, 2002). The crops grown in the Tadla are primarily grains, pulses and sugar beets. Figure 2 illustrates the geographic location of the Tadla's irrigated perimeter within Morocco.

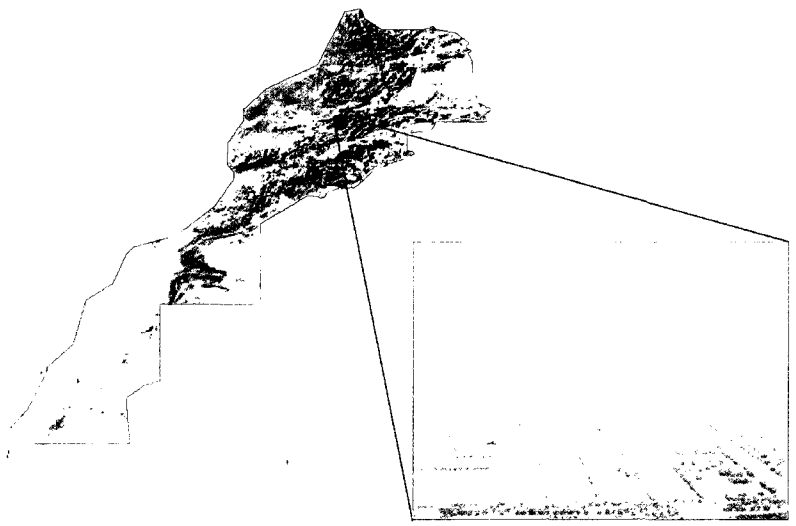

Figure 2: Study site, Tadla's irrigated agricultural perimeter (Béni-Mellal, Morocco)

Since 1954 the sub-perimeter of Béni-Moussa has used water from the Bin-El-Ouidane dam which is generally of good quality (0.3 g/l of calcite, halite and gypsum), while Béni-Amir has been irrigated since 1938 with water from the Oum-El-Rbia river, which has a salinity level of 2 g/l (predominantly calcite and halite). Historically, the development of water resources in the irrigated region of the Tadla has gone through two periods: the first, from

1938 to 1980, was characterized by abundant surface water. The second period started in 1981 with a drought that has continued to this day and led to a considerable lack of water (Badraoui *et al.*, 1998).

With low annual precipitation rates, which are now less than 350 mm, and annual evapotranspiration evaluated at about 1800 mm, the Tadla perimeter has become a semi-arid region. The use of ground water from the underground aquifer has therefore become essential, even if this water is of poor quality (Hammani *et al.*, 2004). This use has lead to an increase in the level of contamination of salinity and sodicity in significant areas of the perimeter (ORMVAT, 2004). Figure 3 gives a sample of four different soils found in the Tadla, including those contaminated with salinity and sodicity.

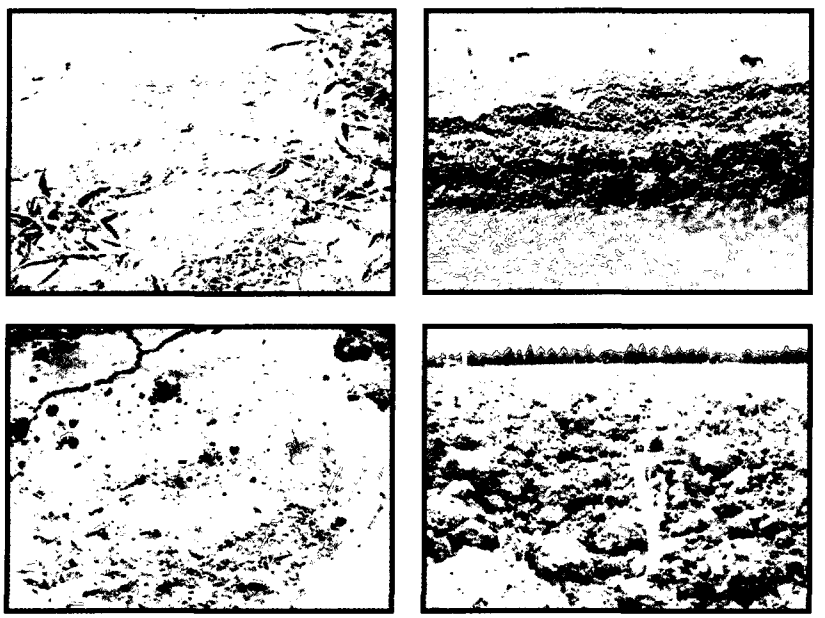

Figure 3: Different soils found in the tadla including (a) saline soils; (b) saline deposit on stream bed; (c) sodic soil; (d) non-contaminated soil with good structure

2.2 ALI image

The Advanced Land Imager (ALI) sensor is on board the American satellite EO-1 which was put into orbit in November 21st, 2000 (NASA, 2006). NASA launched the EO-1 satellite as part of a technology validation/demonstration mission. It has both a multi-spectral sensor (ALI) and hyperspectral capabilities (Hyperion). It follows a repetitive, circular, sun-synchronous, near-polar orbit with a nominal altitude of 705 km at the equator. The ALI is a multispectral instrument which was developed in order to validate the Landsat missions and so follows the same orbit as Landsat 7 in order to obtain cross comparisons, trailing it by roughly a minute. ALI has ten spectral bands ranging from the visible through the near and shortwave infrared, and each image covers a territory of 37 km by 42 km. ALI is a pushbroom instrument, which means that the spectral response from each unique detector will correspond to an individual column of pixels (NASA, 2006). It provides a ground sample distance in the visible and infrared bands (bands 2-10 as seen table 1 and figure 2) of 30 meters which is similar to Landsat. Band 1 is a higher resolution (10 meter) panchromatic band. Table 1 and figure 4 presents the EO-1 ALI bands and the wavelength for each channel.

Table 1: Spectral bands of EO-1 ALI sensor

Band	Wavelength (nm)	Band	Wavelength (nm)
1*	480 – 690	6	775 – 805
2	433 – 453	7	845 – 890
3	450 – 515	8	1200 – 1300
4	525 – 605	9	1550 – 1750
5	630 – 690	10	2080 – 2350

* Panchromatic band

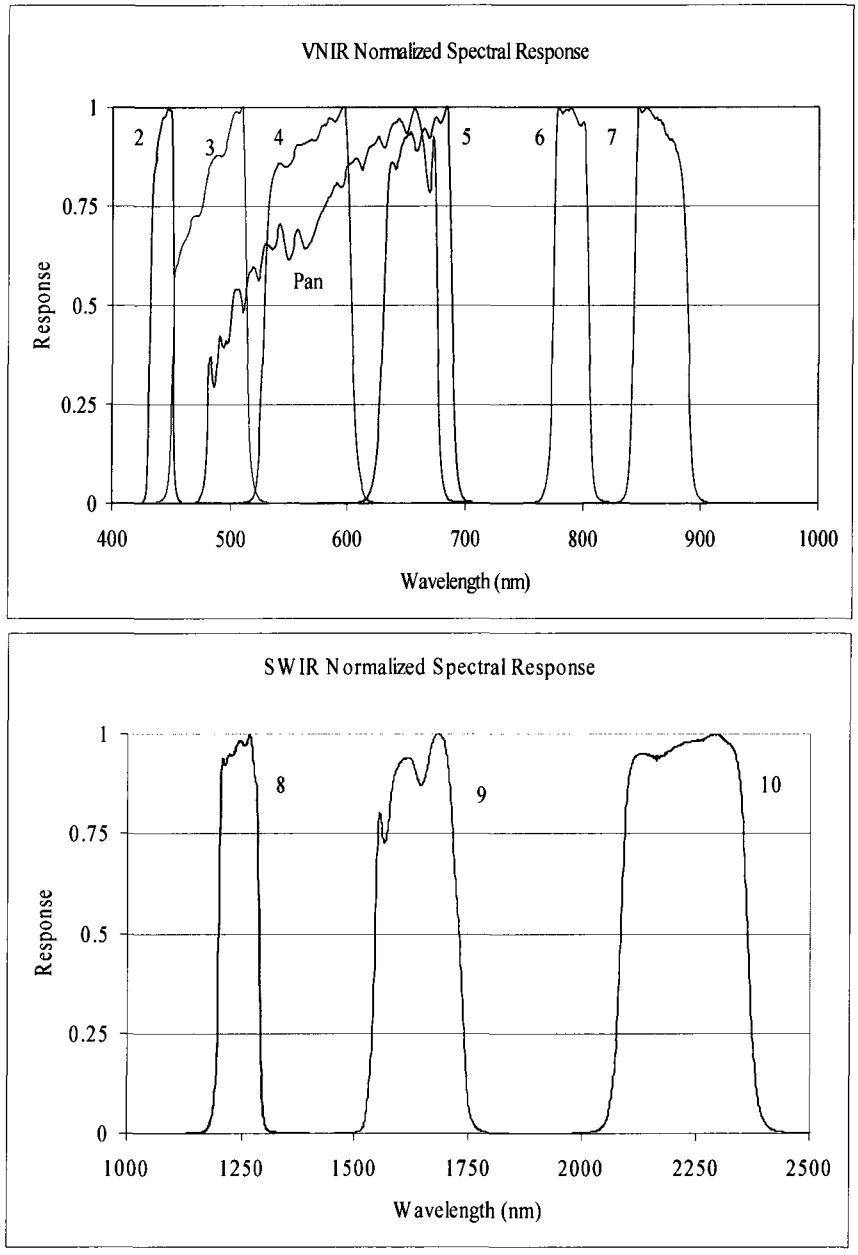

Figure 4: VNIR and SWIR normalized solar-reflective spectral response profile of ALI (EO-1) sensor

The image data for this study was acquired by the ALI sensor on October 1st, 2007, over our study site during the end of the agricultural season in order to have the minimum of vegetation and the largest amount of exposed bare soil to the field of view. Figure 5 shows the original ALI image and the subset image taken of the tadla region and used for the analysis.

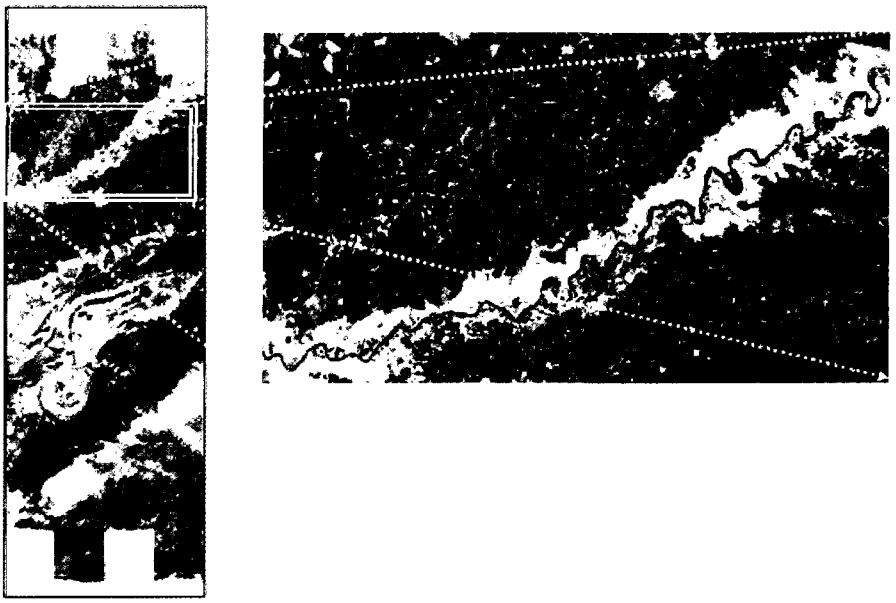

Figure 5: ALI image of Tadla irrigated perimeter (Beni-Mellal, Morocco)

2.3 Data preprocessing

Drift of the sensor makes radiometric calibration (relative and absolute) a necessary step consisting of correcting artifacts affecting the sensor in order to extract precise and reliable information from an image (Bannari *et al.*, 1999). Relative calibration is a normalization and harmonization of the data received from the different detectors of ALI sensor. This step corrects any stripping effects caused by the detectors sensitivity differences (NASA, 2006). Absolute calibration allows the transformation of the digital number, which is measured at the top of the atmosphere, into apparent equivalent radiance. Without these two operations, the changes caused by artifacts relative to the sensor can be mistakenly attributed to changes in the land use and ground biophysical components. Consequently, errors can propagate in all subsequent steps taken during the image processing such as spectral indices calculations, multi-temporal analysis, classification, etc. (Price, 1987 ; Teillet *et al.*, 1994 ; Bannari *et al.*, 1999). The values of the gain and offset, the absolute calibration coefficients, and the solar exoatmospheric spectral irradiance values were delivered with the image by NASA.

Atmospheric effects are dominated by two processes that are responsible for the modification of the satellite signal, mainly absorption by gases (ozone, water vapour, and

CO_2) and diffusion by aerosols and molecules (Deschamps *et al.*, 1981; Kaufman, 1988). These phenomena cause an attenuation of the signal in the direction of illumination, but increase the signal in the other directions because of a diffusion effect. An accurate correction of atmospheric effects requires *a priori* knowledge of the atmospheric parameters that interfere with the data acquisition during its operation (Tanré, 1982). These parameters were measured during the passage of the satellite over the study site, on October 1, 2007, by the meteorological station located closest to the study site. The updated Herman transfer radiative code, H5S (*Simulate the Satellite Signal in the Solar Spectrum*, Teillet and Santer, 1991), was used for atmospheric corrections. H5S simulates the signal measured at the top of the atmosphere from the Earth surfaces reflecting solar and sky irradiance at sea level while considering the sensor characteristics such as the profile of the solar-reflective spectral bands (see figure 4), satellite altitude, atmospheric condition, atmospheric model, Sun and the sensor geometry, terrain elevation, etc. In order to preserve the radiometric integrity of the image, drift of the sensor radiometric calibration and atmospheric effects (scattering and absorption) were combined and corrected in one step (Richards, 1993; Teillet, 1992) using the following equation (NASA, 2006):

$$\rho^*(\lambda) = \frac{L^*(\lambda)\,\pi\ D^2}{Es(\lambda)\ Cos(\theta s)}$$

Where:

$\rho^*(\lambda)$ = Apparent reflectance at the sensor level,

$L^*(\lambda)$ =Radiance at the sensor level,

D = Earth-sun distance in astronomical units,

Es (λ) = Solar irradiances,

θs =Solar zenith angle.

2.4 Salinity indices

Different spectral indices have been proposed in the literature for the detection and identification of saline soils. Khan *et al.* (2001) proposed three spectral indices for the identification of salinity in Pakistan using predominantly bands 3 and 4 of the LISS-II sensor of the IRS-1B platform: the brightness index (BI) (equation 2), Normalized Difference Salinity Index (NDSI) (equation 3) and the salinity index (SI) (equation 4). Of these three indexes, the authors found that the NDSI showed the most promises in the extraction of different salinity classes in a semi-arid environment using satellite data and ground truth data.

Using ground based spectral data, Al-Khaier (2003) developed the salinity index ASTER-SI using bands 4 and 5 of the ASTER sensor (equation 5). It was reported to detect with precision the agricultural salinity phenomenon in semi-arid irrigated agricultural regions of Syria.

A cooperative project between India and the Netherland (IDNP, 2003) also proposed a methodology for the cartography of soil salinity and waterlogging in irrigated cropped land in a semi-arid region of India. After analyzing different remote sensing techniques, this project recommended three different salinity indices using Landsat 5-TM Bands 4, 5 and 7 : SI-1 (equation 6), SI-2 (equation 7) and SI-3 (equation 8). These indices were developed using surface radiative properties data, biomass depression and moisture indicators.

Using the simulated data of soil reflectance, Bannari *et al.* (2008) demonstrated that the short wave infrared is more sensitive than other bandwidths to different degrees of salinity and sodicity, especially for low and medium levels of salinity. They proposed two indices: Soils Salinity and Sodicity Indices 1 (Equation 9: SSSI-1) and 2 (Equation 10: SSSI-2). These indices appear to increase the precision of identification and be particularly well suited to the identification of low and medium levels of salinity and sodicity using simulated ALI sensor data. The considered indices to be tested and analyzed in this research are summarized below in table 2.

Table 2: Indices described in literature and considered in this study

INDEX	*EQUATION*	*SENSOR*	*AUTHOR and AREA*
(2) BI	$\sqrt{ALI5^2 + ALI6^2}$	IRS-1B LISS-II	Khan *et al.* (2001) Pakistan
(3) NDSI	(ALI 5-ALI 7)/(ALI 5+ALI 7)	IRS-1B LISS-II	Khan *et al.* (2001) Pakistan
(4) SI	$\sqrt{ALI3 * ALI5}$	IRS-1B LISS-II	Khan *et al.* (2001) Pakistan
(5) ASTER-SI	(ALI 9-ALI 10)/(ALI 9 + ALI 10)	ASTER	Al-Khaier (2003) Syria
(6) SI-1	(ALI 9)/(ALI 10)	Landsat 5-TM	IDNP (2002) India
(7) SI-2	(ALI 6-ALI 9)/ (ALI 6+ALI 9)	Landsat 5-TM	IDNP (2002) India
(8) SI-3	(ALI 9-ALI 10)/(ALI 9+ALI 10)	Landsat 5-TM	IDNP (2002) India
(9) SSSI-1	(ALI 9 - ALI 10)	EO-1 ALI	Bannari *et al.* (2008) Morocco
(10) SSSI-2	(ALI 9*ALI 10 –ALI 10*ALI 10)/ALI 9	EO-1 ALI	Bannari *et al.* (2008) Morocco

The bands used in the equations of the considered indices, when developed for sensors other than ALI, were replaced with the equivalent bands from the ALI sensor before any manipulation of the data was done. In order to test the indices potential to detect low and moderate levels of salinity using the ALI spectral bands, two different and independent sources of data were used. Ground spectroradiometric measurements and laboratory analysis were used to develop semi-empirical models. Then, the models were applied to the ALI image and validated to the ground truth.

2.5 Semi-empirical models

The soil samples were collected during the dry season between the 25th of August and the 5th of September 2005. The samples collected are considered representative of the soils found in the region with varying levels of salinity and sodicity. The soil samples were taken from the top 5 cm of soils and observations and comments on the soils appearance were noted for each sample. The descriptions of the soil samples and related comments can be found in Bannari *et al.* (2008). The position of each sample was taken using a GPS (with a

precision of ±3 à ±5 m) and photographs were taken using a digital camera.

Laboratory analyses were conducted on each sample measuring the electrical conductivity (E.C.) extracted from saturated paste (measure of salinity) and the pH (an indication of sodicity). These analyses were done in the ORMVAT laboratory in Morocco using methods set forth according to the international standards in soil science (Baize, 1988). Each sample of soil is characterized by its own structure, texture, mineral composition, level of salinity and sodicity etc., resulting in a distinct particular spectral signature in the different wavelengths of the electromagnetic spectrum. These chemical analyses bring to light the impact of salinity and sodicity on the soils spectral signature and allow the soils to be classified according to the matrix put forth by Metternicht and Zinck (1997) that classifies soils according to salinity and sodicity.

Before the samples were analyzed in the laboratory, spectroradiometric measurements were taken using an ASD (Analytical Spectral Devices, 1999) spectroradiometer which has the capacity to sample continuously the reflectance in the visible and infrared (350 to 2500 nm) with a sampling interval of 1.4 nm in the 350 to 1000 nm region of the spectrum and an interval of 2 nm in the 1000 to 2500 nm region of the spectrum. The spectral behaviours of the soils confirmed that the higher the levels of salinity and sodicity in the soil, the higher the reflectance in the infrared spectral bands (Metternicht and Zinck, 1997; Mougenot *et al.*, 1993: Joshi *et al.*, 2002), salinity and sodicity being considered here as a single variable.

The spectral signatures of the soil were re-sampled and convolved in the ALI bands; the data confirms that the infrared part of the spectrum, especially bands 9 and 10, provides the greatest differentiation between signatures. The simulated reflectance data in ALI spectral bands were used in the calculation of the different indices described earlier. Semi-empirical models were derived using second order regression analyses between the E.C. and the different spectral salinity indices calculated from ground spectroradiometric measurements. A detailed description of all the steps leading to the development of the semi-empirical models can be found in Bannari *et al.* (2008).

The second order regressions mentioned above were done using first all of the soils, then only soils with some level of salinity and sodicity. The choice to use the second order regression was based on results published by Bannari *et al.* (2008) that indicated that the second order regression provides the highest performing statistical relationship for the Tadla

soils.

Table 3 presents the result of the second order regression using the list of published indices as well as the derived predictive model. The resulting correlation coefficients (R^2) are calculated at 95% confidence interval.

Table 3: Correlation coefficient between E.C. and spectral soil salinity indices at significance level $p< 0.005$.

Salinity indices	All considered soils	Only soils with salinity and sodicity
SSSI-1	y = 1E-05x2 + 0,0026x + 0,0096 R^2 = **0.58**	y = -9E-05x2 + 0.0046x + 0.0013 R^2 = **0.96**
SSSI-2	y = -2E-05x2 + 0,0023x + 0,0111 R^2 = **0.56**	y = -9E-05x2 + 0.0042x + 0.0017 R^2 = **0.96**
NDSI	y = 0,0038x2 - 0,0432x - 0,0779 R^2 = **0.70**	y = 0.0011x2 - 0.0202x - 0.097 R^2 = 0.42
BI	y = 0.0028x2 - 0.0289x + 0.2894 R^2 = 0.23	y = -0.0003x2 + 0.0058x + 0.2261 R^2 = 0.05
SI-1	y = -0.0041x2 + 0.0465x + 0.9963 R^2 = 0.31	y = -0.0006x2 + 0.0166x + 1.003 R^2 = **0.7852**
SI-2	y = -0.0025x2 + 0.0265x - 0.353 R^2 = 0.14	y = -0.001x2 + 0.0055x - 0.3004 R^2 = 0.24
SI-3	y = -0.0018x2 + 0.0207x - 0.0002 R^2 = 0.33	Y = -0.0003x2 + 0.0079x + 0.0019 R^2 = **0.7869**
SI-ASTER	y = -0.0018x2 + 0.0207x - 0.0002 R^2 = 0.33	Y = -0.0003x2 + 0.0079x + 0.0019 R^2 = **0.79**
SI	y = 0.0023x2 - 0.0252x + 0.1522 R^2 = 0.43	Y = 0.0003x2 - 0.0039x + 0.1179 R^2 = 0.04

*p-values in the table are significant at a p=5/10 level of rejection and take into account the Boneferroni correction for multiple tests

As noted above, the indices were tested both with all considered soils (affected and non-affected) and with only affected soils. The soils retained, when the number of soils was reduced, were saline soils with low or moderate levels of sodicity. Diminishing the number of soils samples, in the case of certain indices, substantially improved the correlation coefficient and therefore the ability to predict the salinity conditions in the Tadla region. Not all the models generated proved to provide a significant correlation. This may be due to several reasons: First, most of the indices used to generate the models were not developed for the ALI sensor and may therefore not translate well into the ALI bands. Second, the fact

that most of the indices were developed for areas other than the Tadla may contribute to the absence of an effective correlation since these indices were developed to detect kinds of soils, or a specific regional profile of soils, which may not easily match the types of soil found in the Tadla.

Only those models which were found to have a high R^2 were retained for further analysis. Complete reliance on a high R^2 value is insufficient, however, since a high value for R^2 does not guarantee that the model will be able to accurately map salinity once applied to the image. Those models producing the statistically strongest relationship have to be therefore subjected to more rigorous testing once applied to an image, and only those which produce good results during the validation procedures are considered as potentially acceptable final models.

3. RESULTS ANALYSIS

Of all the suggested models, 5 were retained as being sufficiently correlated with the E.C. (R^2 of more than 0.70) of the soil and were then applied to the image and analyzed. The equations for the retained models, including the R^2, are found below in table 4.

Table 4: Summary of the regression models tested on the image and the R-squared

Salinity indices	Semi-empirical models	R^2
NDSI	y = 0,0038x2 - 0,0432x - 0,0779	**0.70**
SI-1	y = -0.0006x2 + 0.0166x + 1.003	**0.79**
SI-ASTER (SI-3)	y = -0.0003x2 + 0.0079x + 0.0019	**0.79**
SSSI-1	y = -9E-05x2 + 0.0046x + 0.0013	**0.96**
SSSI-2	y = -9E-05x2 + 0.0042x + 0.0017	**0.96**

Among the indices proposed, the highest correlation using all considered soils (affected and non-affected) was obtained with the NDSI (70%). The model derived from NDSI is the only one retained based on all considered soils. The SSSI-1 (58%) and the SSSI-2 (56%) achieved even better correlations when using only affected soils (96% for both SSSI-1 and SSSI-2) so it is these models which were retained for analysis. Again, the results support the finding of Bannari *et al.* (2008) and confirm that the SSSI-1 and SSSI-2 give us the highest correlation considering all soils or only affected soils.

The retained models were applied to the corrected image using PCI Geomatica and the EASI modeling function. The single output channel was then analyzed in pseudocolor transformation. Once the selected models were applied to the ALI image, validation was done in two ways:

1) A visual analysis of the derived maps was done to get a sense of the models performance when compared to the ground truth map. The visual analysis was based on the overall similarity of the derived maps to the ground truth and also the analysis of several key regions of both maps.
2) A statistical analysis was conducted by taking pixels from the derived salinity maps and comparing those values to the levels of E.C. of an equivalent point from the validation map.

Both statistical analysis and visual analysis are related in that both are comparisons between the values produced by the models to derive salinity maps, and the validation map, which is considered to be representative of the ground truth. A map of E.C. produced by the ORMVAT based on chemical analysis and GIS was considered to be representative of ground truth (figure 6), since E.C. is considered an accurate measure of salinity.

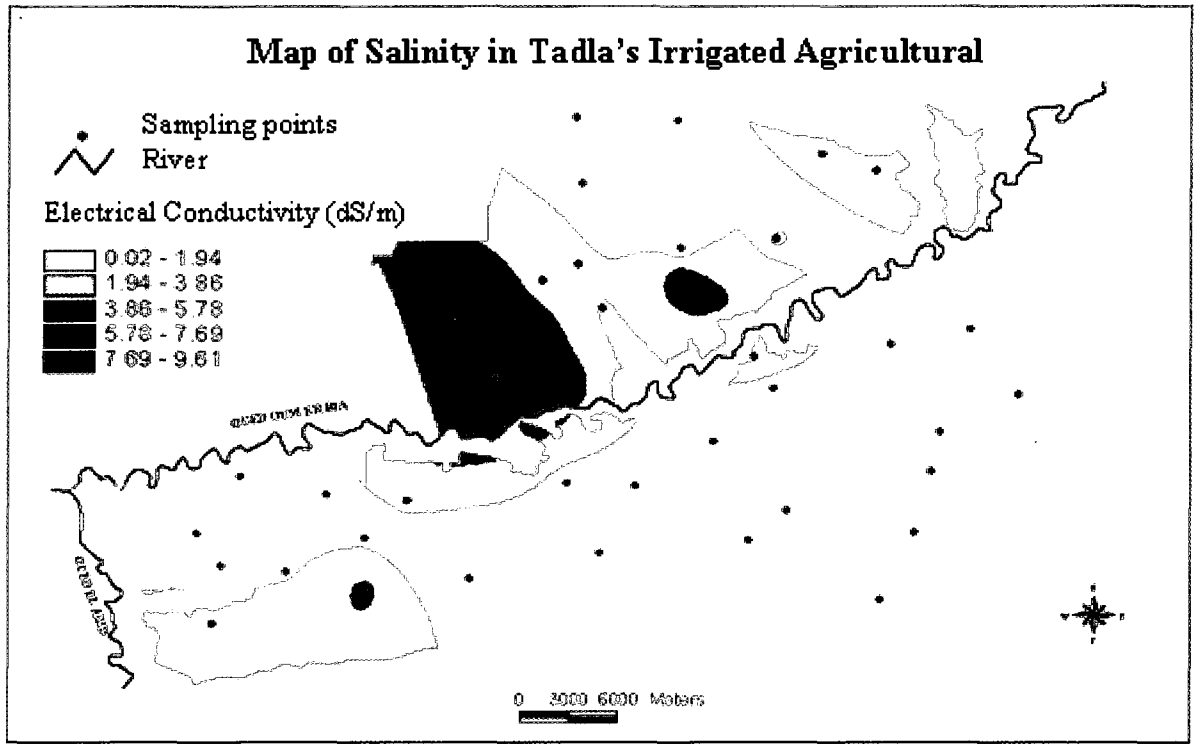

Figure 6: Map of salinity in Tadla's irrigated agricultural perimeter (Béni-Mellal, Morocco) (Source: ORMVAT, 2004)

The ORMVAT map gives us five classes of salinity, however 0.02 to 1.94 and 1.4 to 3.8 are both below 4 ds/m and so would both be considered non-saline. It is on the basis of these classes that the analysis of the model derived maps are evaluated. Since pH was not considered as a variable for the establishment of the ORMVAT map, the levels of sodicity cannot be validated. Only salinity can be considered in the remainder of the analysis, being understood that both conditions tend to occur together in this region and the presence of salinity is predictive of the presence of sodicity.

One of the criteria for a well performing model should be the correspondence of the image values to the classes present on the validation map. It bears keeping in mind that the ORMVAT map was produced using interpolation techniques and data from only 40 soil

quality monitoring sites (ORMVAT, 2009). This cartographic generality means that some realities on the ground are glossed over and precision can be lost. In addition, a well performing model will have the higher values found in areas that the validation map suggest have higher salinity levels and lower values corresponding to non-saline areas. There should also be differentiation between the various levels of salinity present and a minimum of confusion between saline soils and vegetates and/or non-saline areas.

The goal of the visual analysis is to find the model that represents as accurately as possible the low and mid-level of salinity present in the Tadla region.

Certain areas on the ORMVAT map were targeted because they are easily identifiable on the ALI salinity map and they correspond to different levels of salinity. In the case of ALI salinity map of the Tadla there are a few areas that are key references to the analysis, mainly the areas of slight and moderate salinity which are essential for the analysis as well as an area reported to be non saline for comparison. Although each of the models applied to the image was found to have a significant correlation to the E.C., it is evident when looking at the images produced by application of the models that there are not all equally precise. A final validation procedure was undertaken in order to confirm the results of the visual analysis. Since we already had the visual interpretation of the images that were ground checked, we were able to recognize pixels that represented the classes. Pixels were selected from the different areas of the image and their values were then compared to the E.C. values given by the corresponding areas in ORMVAT map. The pixels were selected from the same key areas of the maps that were used for the visual analysis, choosing those in particular which seemed to be part of the visually dominant class in that area and making sure to have a sample representative of the E.C. classes on the validation map. The values obtained from the pixels were then correlated with the E.C. values from the validation map using a second order regression. Because the E.C. map is based on an extrapolation, the validation was conducted keeping in mind that we are looking for the model which gives the best overall performance, so only pixels which were dominant in an area were selected.

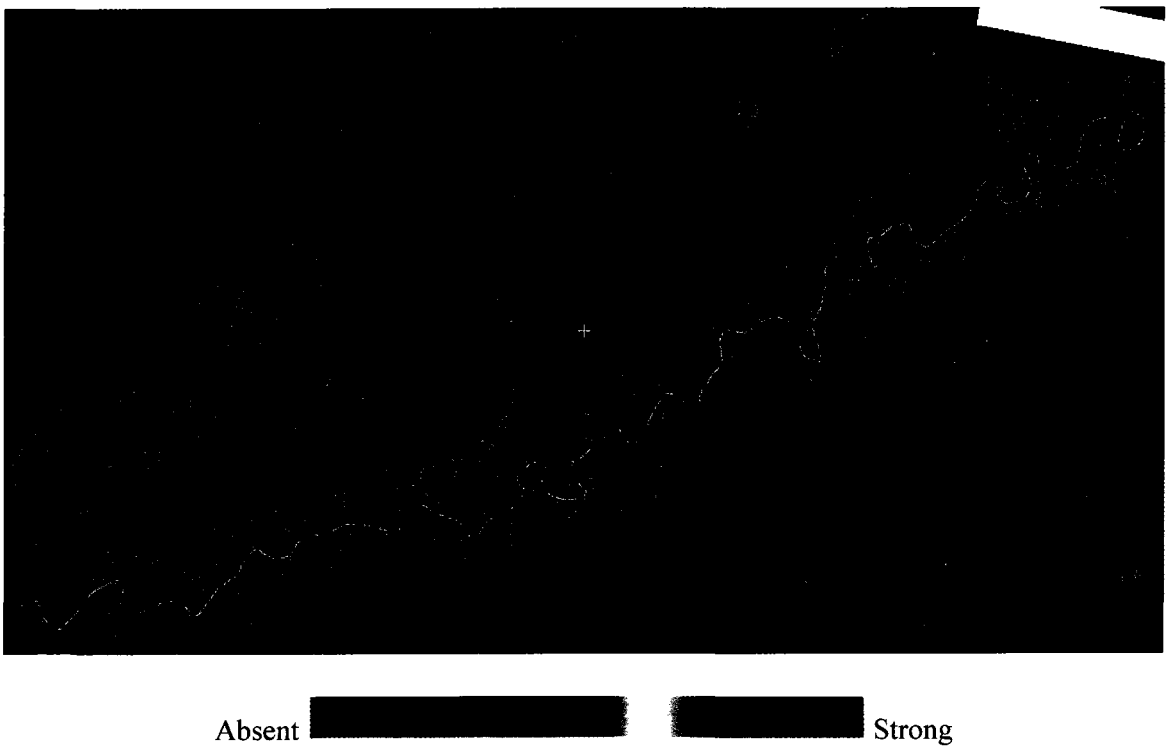

Figure 7: Map of salinity derived using the model based on the NDSI index

Despite the significant correlation between the E.C. of soils from the ground truth and the model based on NDSI (figure 7), the model derived does not accurately map regions of salinity and sodicity. Indeed, the NDSI derived model does not require any validation because the map it produced indicates that the entire region is void of salinity and sodicity, which we know not to be the case based on the validation map and chemical analysis of the soils. The difficulty may stem from the fact that the model generated from the NDSI index is based on non-contaminated soils as well as contaminated soils, which could be preventing it from properly identifying saline and sodic soils. In addition, NDSI was not developed based on ground truth measurements or any correlation, but rather was an empirical model based on image data.

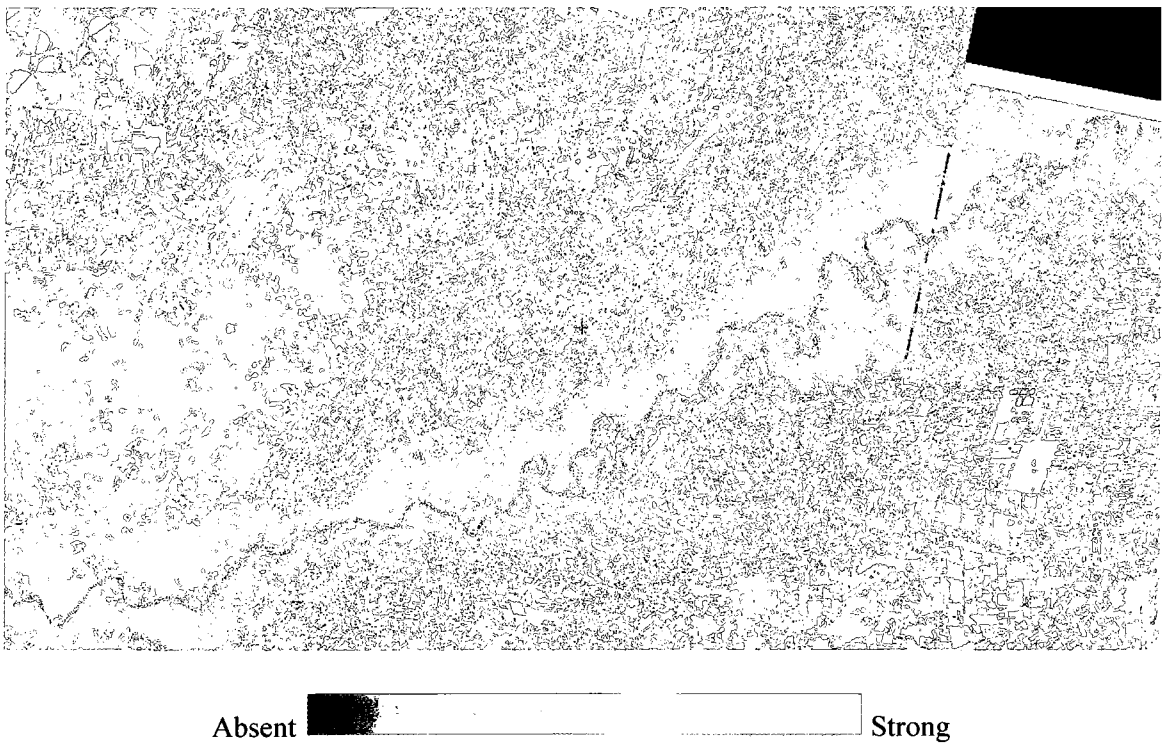

Figure 8: Map of salinity derived using the model based on the SI-1 index

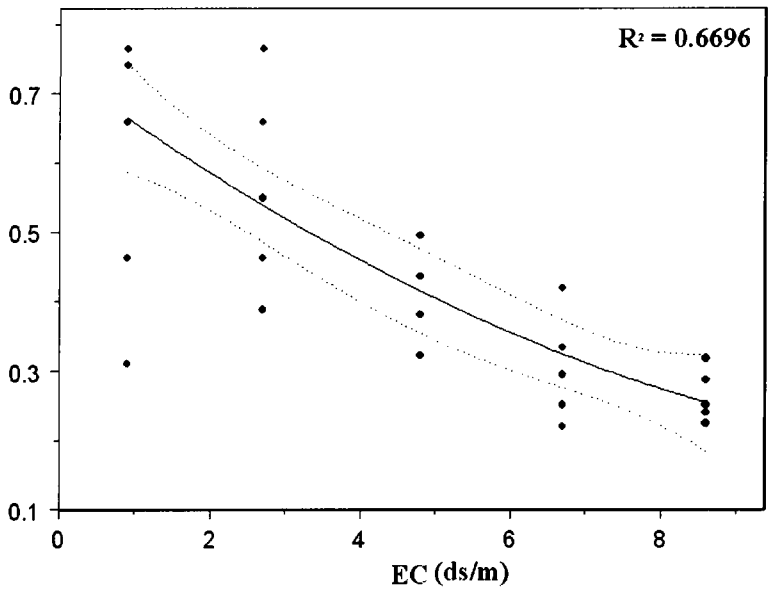

Figure 9: Relationship between E.C. (ground reference) and different salinity classes derived from ALI image using model based on SI-1 index

The SI-1 model (figure 8) seems to have only 3 dominant classes: strong, medium and slight salinity. However, the strong class does not accurately reflect the ground truth because in this area there is no salinity (see validation map) just vegetation. Therefore, the vegetation is being detected as high salinity bare soil as apparent from the well delineated agricultural fields which appear in bright red

The statistical validation (figure 9) produces an R^2 of 0.67. This low value reinforces what is seen visually. The area of medium salinity is well identified, but not the areas known to be non-saline. The scatter plot further shows that the problem is linked to the fact that the different salinity classes are poorly differentiated.

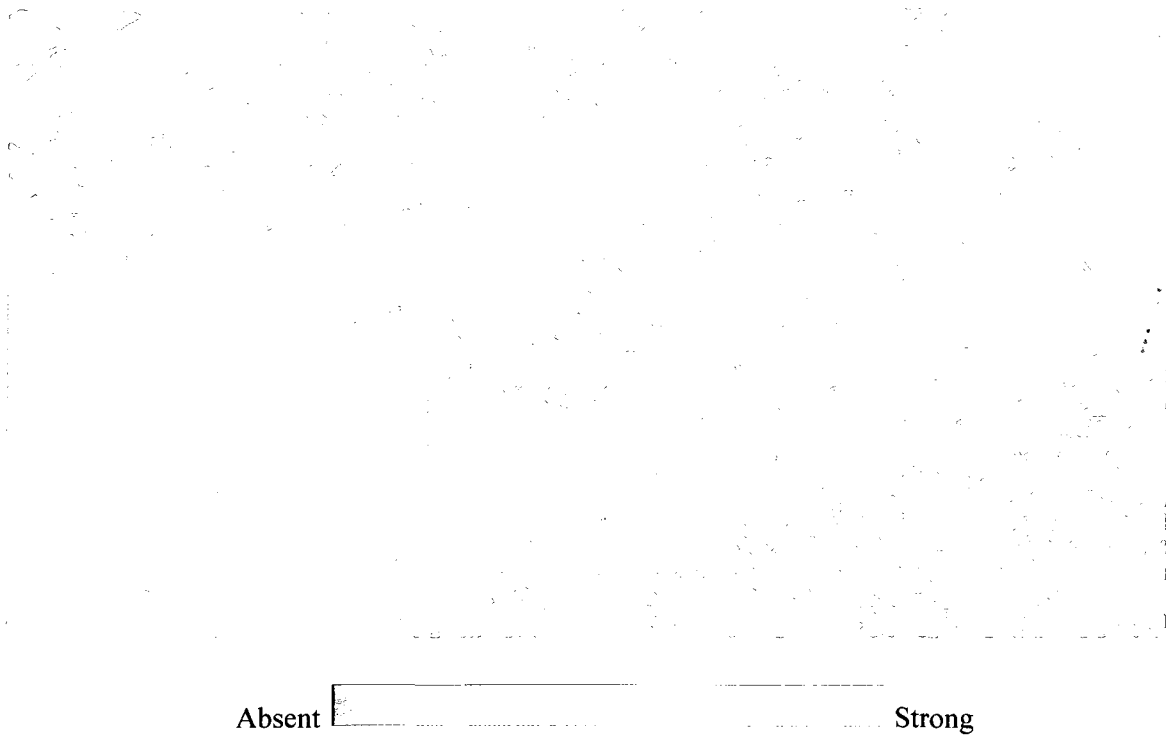

Figure 10: Map of salinity derived using the model based on the SI-ASTER index

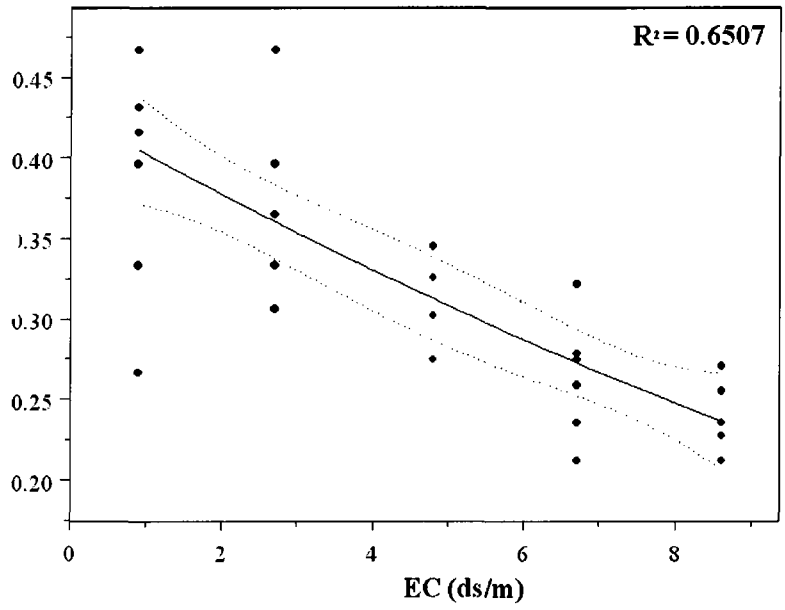

Figure 11: Relationship between E.C. (ground reference) and different salinity classes derived from ALI image using model based SI-ASTER (SI-3) index.

The SI-ASTER (Figure 10) appears to produce the same three dominant classes as the SI-1 and does not indicate the there is salinity in certain areas which the validation map clearly indicates should be present. The SI-ASTER model presents much the same behaviour as the SI-1 with the areas of moderate salinity being well delineated, but the vegetation being mistaken for high salinity by the model. The effect is less pronounced that with SI-. The statistical validation (figure 11) produces an R^2 of 0.65 which is the lowest of all tested model, and closer examination of the scatter plot reveals that the classes are poorly differentiated in much the same was as the SI-1

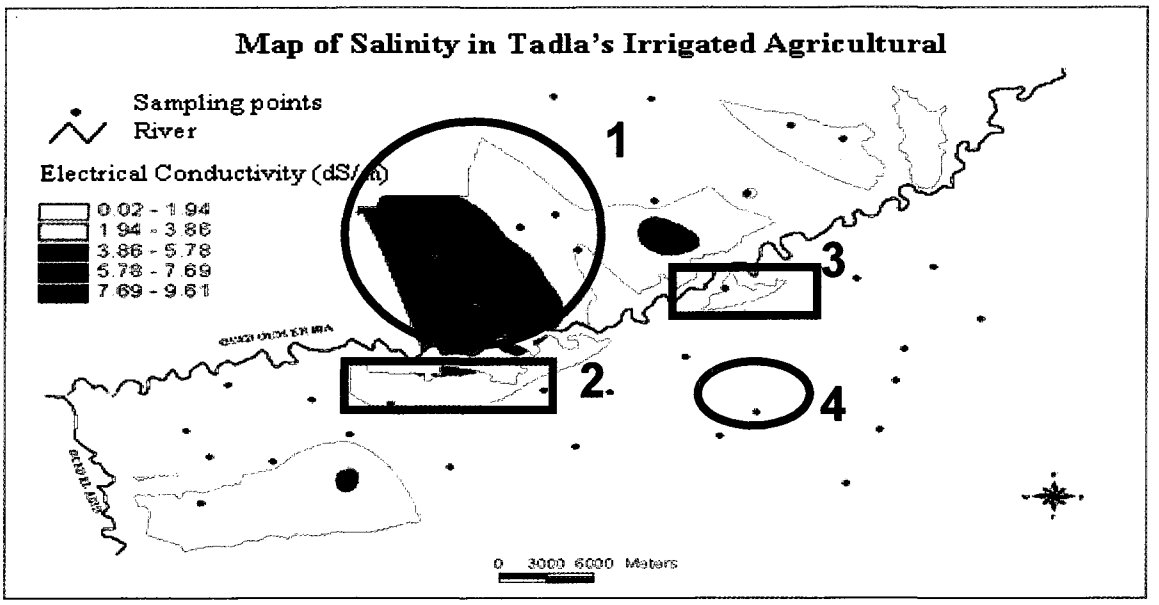

Figure 12: Key areas of E.C. used for the validation of SSSI models

The models based on the SSSI indices give a more visually varied response so to make the analysis a little easier it will focus on four well defined areas which are shown in figure 12. The area of higher salinity in the middle of the area (1) which was seen in the SI-1 and the SI-ASTER, as well as an area of lesser salinity (2) on the other side of the river. There are also two areas considered non-saline in order to test the model's sensitivity to both saline and non-saline soils. Though (3) is considered to be non-saline, is still has an E.C. higher than zero and it would be useful to have an idea of areas where salinity is developing. Though the models were not developed with any soils under 4 ds/m, it would be an added advantage if they were able to make this additional differentiation. The map indicates that the final area (4) is non-saline completely. These 4 areas represent the different conditions of salinity found in the Tadla, and in order to be considered precise, the models must be able to tell the difference.

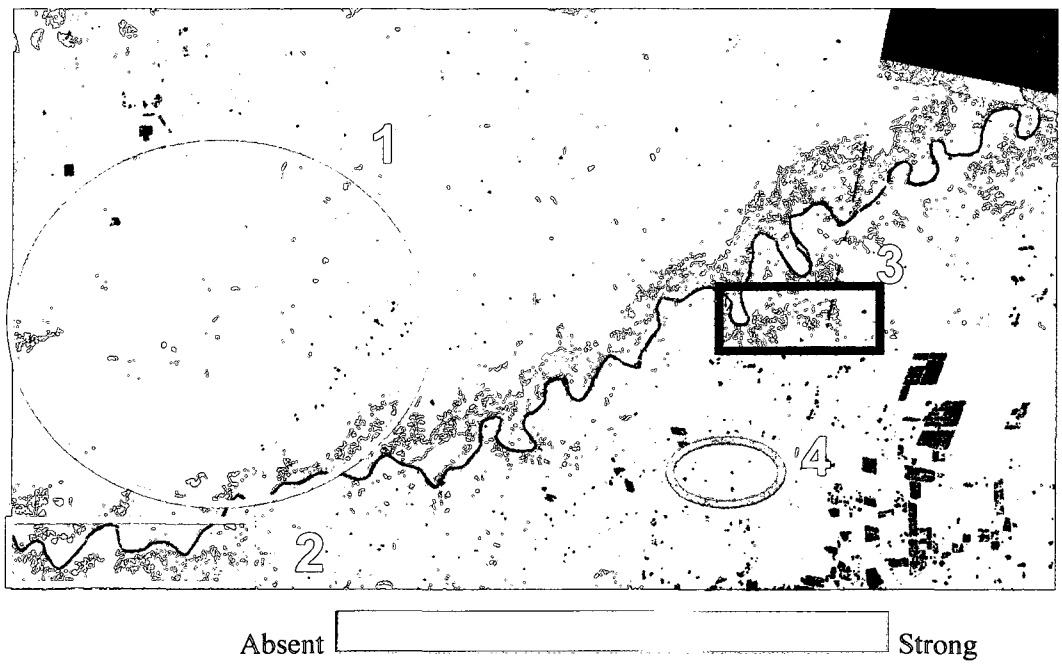

Figure 13: Map of salinity derived using the model based on the SSSI-1 index

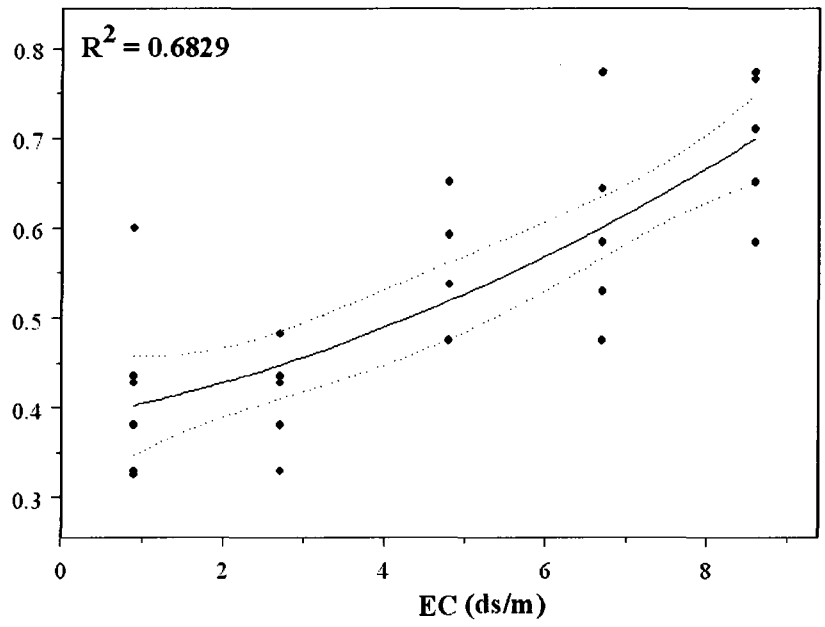

Figure 14: Relationship between E.C. (ground reference) and different salinity classes derived from ALI image using the model base on the SSSI-1 index

The model based on the SSSI-1 index (figure 13) performs better than the other models based on the SI-1 and SI-ASTER indices in that it give us more that three classes and visually gives a more refined picture of the ground truth. Contrary to the other models, the areas considered non-salinity (4) are accurately represented, as is the region of low salinity (2) however, area 3, which the validation map tell us has salinity below 4 ds/m is showing the same response as area 2, which should be exhibiting a higher response. Finally, area 1 which should be displaying some of the highest values on the map is showing only the more moderate levels of salinity. The scatter plot (figure 14) validates the visual analysis since despite the fact that there seems to be more refinement to the derived map visually, the R^2 is only 0.68. We see that the points chosen in the areas with salinity under 4 ds/m are considered as one class, which is consistent with the fact that the model was not developed to detect salinity lower than that. Another problem becomes obvious in the moderate salinity range, where the salinity class between 6 and 8 actually seems to give an average value slightly lower than the class of between 4 and 6. The scatter plot also shows that the model

does not differentiate well between the higher salinity class and the moderate salinity classes.

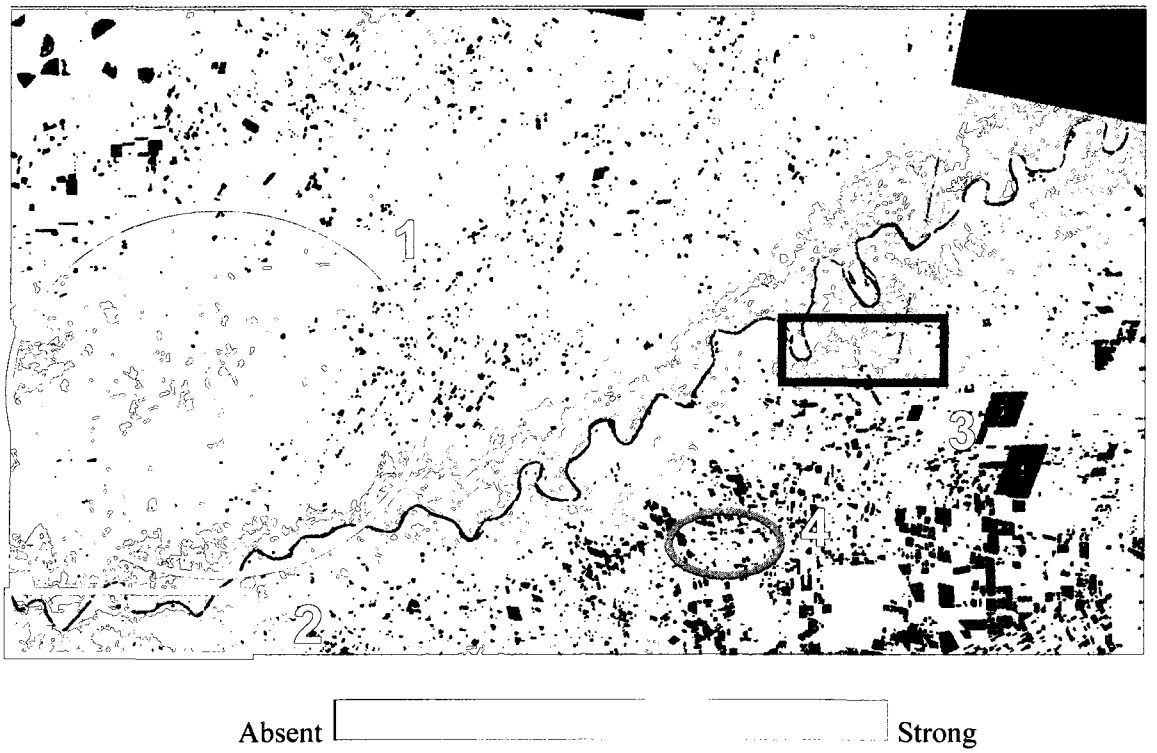

Figure 15: Map of salinity derived using the model based on the SSSI-2 index

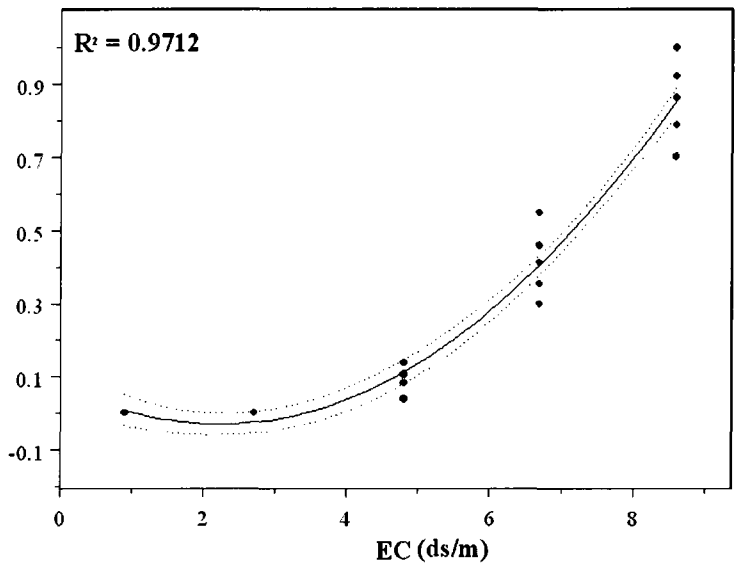

Figure 16: Relationship between E.C. (ground reference) and different salinity classes derived from ALI image using the model based on the SSSI-2 index

The model based on the SSSI-2 index (figure 15) is clearly the model which gives the best results. It is the map which gives the closet overall visual approximation to the validation map. Area 1 is identified as an area of medium salinity and there are also quite a few points which indicate the core of higher salinity which is located in that area. The higher salinity in area 2 is also present. The same difficulty surrounding having the same values for area 2 and area 3 are still found, but it is less pronounced than with the SSSI-1. Finally, non-saline areas (4) are shown to be non saline by the model. Visually, this model is validated as being at least as accurate at the extrapolated E.C. map. Statistical validation (figure 16) of the SSSI-2 model has an R^2 of 0.97, which is by far the highest of any of the other models. Analyzing the scatter plot, we see that the different classes are well separated out, which further reinforce the results of the visual analysis.

4. CONCLUSION

Different semi-empirical modelizations based on salinity indices were developed using the spectral signature of saline and sodic soils collected from the Tadla irrigated perimeter in Morocco, the E.C. of these soils and the spectral bands of the EO-1 ALI sensor. Semi-empirical predictive models were derived using a second order statistical regression and applied to the image of the study area. The derived maps were analyzed, both visually and statistically, using a map of the E.C. which is considered to represent the ground truth for validation, in order to see which model would be well suited to the characterization and mapping of soil salinity and sodicity in the Tadla's irrigated perimeter in Morocco.

The model based on the NDSI index does not give any results, the map created being almost completely black. The models based on the SI-1 and the SI-ASTER (SI-3) indices show vegetation as being high salinity soils, though the model does bring out areas of lower salinity. The R^2 of 0.67 for the SI-1 and 0.65 for the SI-ASTER (SI-3) further reinforce the finding that these models present too much confusion between the classes to be used with any accuracy. The model based on the SSSI-1 index is visually better than the SI-1 and SI-ASTER (SI-3) in that it give us more that three classes and visually gives a more refined picture of the ground truth. However, there is confusion between the classes in the mid-levels of salinity, and the higher classes of salinity do not appear in areas where the validation map asserts the presence of higher levels of salinity. The statistical validation reinforces what is seen on the image with an R^2 of only 0.68. By contrast, the model based on the SSSI-2 index is clearly the model which provides the best results in comparison to the validation map. It is the map which gives the closet overall visual approximation of the visual map, with a whole range of values. With a statistical validation of $R^2 = 0.97$, it is by far the best performing of any of the models, with the different classes of soil being statistically well separated out, which further reinforces the visual analysis. The models that use the ALI bands 9 and 10 are those that most accurately corresponding to the areas of salinity as mapped by the ORMVAT map created by GIS and statistical methods.

II. CONCLUSIONS

The goal of this study was to test a remote sensing technique that could allow for the mapping of moderate salinity and sodicity with at least as much accuracy as traditional methods, but without the higher costs associated with them. In addition, this study represents the first known attempt to use the EO-1 ALI sensor for the detection of soils salinity.

The high correlation between soil reflectance in the SWIR region and the salt and sodium content of soils is the aspect that is exploited in the mapping of affected soils with remote sensing. The analysis of the Tadla soils confirms the spectral behaviour of salinity described in previous studies (Chapman *et al.,* 1989; Hick and Russel, 1990; Rao *et a.*, 1991; Mougenot *et al.,* 1993; Rao *et al.,* 1995; Metternicht and Zinck, 1997; Bannari *et al.*, 2008). In the case of the Tadla soils, when moderate and slight levels of salinity were characterized spectrally, it was confirmed that the higher the salinity and sodicity content in the soils, the higher the reflectance in the SWIR bands. In fact, the SWIR wavelengths provide an expressive means of characterizing saline and sodic soils. However, spectral confusion can often occur between moderate or slightly saline and sodic soils, and non-affected soils with bright and clear color. This spectral confusion can be minimized and soils with slight and moderate salinity can be identified provided certain methodological points are followed:

1 - One of the important aspects of this research was to assess the potential and limits of the EO-1 ALI sensor spectral bands for the discrimination of slight and moderate soil salinity and sodicity. The SWIR region provides a good indicator; it is the most sensitive part of the spectrum to different degrees of soil salinity and sodicity, and the increased precision of that part of the spectrum in the ALI sensor does, as predicted, produce good results for salinity detection.

2 - Testing the various indices suggested in the literature showed that those using ALI bands 9 and 10 give the best results. When taking into account the spectral behaviour of vegetation, salinity indices help to minimize the interference of vegetation and one can further isolate the level of salinity and sodicity present in the soil. While some of the indices were virtually useless when applied to an ALI image of the Tadla region it is important to note that most of these indices were not developed for the ALI sensor. Only the SSSI-1 and the SSSI-2 (Bannari *et al.*, 2008) were developed with the ALI bands in mind, using ground

data from Tadla's irrigated agricultural perimeter and these were shown to perform better than any other indices for this region of Morocco. The model based on the NDSI index did not give any results and the models based on the SI-1 and the SI-ASTER (SI-3) indices showed vegetation as being high salinity soils, though the model did bring out areas of lower salinity. The model based on the SSSI-1 index is visually better than the SI-1 and SI-ASTER (SI-3), however, there is confusion between the classes in the mid-levels of salinity and the higher classes of salinity. The model based on the SSSI-2 index is clearly the model which gives the best results in comparison to the ground truth. It gives the closet overall approximation visually of the validation map, with a whole range of values. Statistical validation further reinforced the visual analysis.

3 - It was found that the use of semi-empirical models based on the E.C. and the specific spectral measurements relative to our study site provides better results than using only spectral bands alone for the identification of saline soils in semi-arid agricultural regions with large areas of bare soil, and for moderate and slight salinity and sodicity to be mapped.

4 – Tests also confirm that better results are obtained if the semi-empirical predictive models are those based on the indices SSSI-1 and SSSI-2. The predictive models were also found to be most successful when derived from a selection of soils which consist of mostly slightly saline and moderately sodic soils.

The ALI sensor does appear to be well suited to the spectral behaviour of the minerals which cause salinity and sodicity. The ground data collected to build the models was specific to the study area and so allowed for a precise modeling of the ground situation in the Tadla. The indices and methodology presented here provide a suggested a starting point for the development of models which could be perfected for other geographical region, however every region would have to refine the process to find the combination of index and model which will effectively map its salinity and sodicity.

The irrigated perimeter of the Tadla in Morocco is only one area among many in the world where salinity and sodicity are an increasingly serious problem. The methodology outlined in this study provides a method which is at least as accurate as traditional methods, but is a more cost effective means for monitoring large areas of agricultural land.

III. RECOMMENDATIONS

This study does suggest some areas where future research would be warranted. First, the ALI sensor has no thermal band, a band some researchers (Mougenot *et al.*, 1993; Verma *et al*, 1994) have found to be particularly useful; it would be interesting to verify whether the development of a salinity index and semi-empirical model which includes a thermal band would increase the precision of soil identification.

Second, though the EO-1 ALI spectral bands are clearly an improvement on Landsat-ETM+, hyperspectral sensors may better suited than multi-spectral sensors for the discrimination of slight and moderate soils salinity and sodicity. Very little research has been done on the use of hyperspectal for soil salinity detection, probably because affordable hyperpectral images are still a relatively recent phenomenon. It would be worthwhile to investigate whether using hyperspectral sensors would bring appreciably improved over multi-spectral sensors in the detection of soil salinity in arid and semi-arid conditions.

In addition, there is insufficient data to indicate whether the methodological model developed in this study could predict salinity in climates other than arid and semi-arid ones, or in areas with vastly different soil characteristics, or higher vegetation cover. Research is necessary to test if semi-empirical predictive models developed in this study are as accurate for other climate or soil types.

Finally, the models developed here have not been tested for areas containing soils with high salinity or high sodicity concentrations.

IV. REFERENCES

Abrol, I.P., Yadav, J.S.P. and Massoud, F.I. (1988) Salt-affected soils and their management, FAO soils bulletin 39, Soil Resources Management and conservation Service FAO Land and Water Development Division, Food and Agriculture organization of the United Nations, Rome. 131 pages.

Al-Khaier, F. (2003) Soil Salinity Detection Using Satellite Remotes Sensing. Master's thesis, International institute for Geo-information science and earth observation, Enschede, The Netherlands. 61 pages.

Analytical Spectral Devices, ASD Inc., (1999) http://www.asdi.com/products-spectroradiometers.asp

Badraoui, M., Soudi, B., and Farhat, A. (1998) Variation de la qualité des sols : Une base pour évaluer la durabilité de la mise en valeur agricole sous irrigation par pivot au Maroc. Institue Agronomique et Vétérinaire Hassan II, Rabat, Maroc : 227-234.

Ben-Dor, E., Patkin, K., Banin, A., and Karnieli, A. (2002) Mapping of several soil propertiesusing DAIS-7915 hyperspectral scanner data. A case study over soils in Israel. *International Journal of Remote Sensing*, 23: 1043-1062.

Baize, D. (1988) Guide des analyses courantes en pédologie: choix expression, presentation et interpretation. INRA, Paris, France. 172 pages.

Bannari, A., Teillet, P.M., and Richardson, G. (1999) Nécessité de l'étalonnage radiométrique et standardization des images numérique de télédétection, *Canadian Journal of Remote Sensing,* Vol. 25(1): 45-59.

Bannari, A., Guedon, A.M., El-Harti, A., Cherkaoui, F.Z. and El-Ghmari, A. (2008) Characterization of Slight and Moderate Saline and Sodic Soils in Irrigated Agricultural Land Using Simulated Data of ALI (EO-1) Sensor. *Journal of Soil Science and Plant Analysis*, vol. 39: 2795-2811.

Bellouti, A., Cherkaoui, F., Benhida, M., Debbarh, A., Soudi, B. and Badraoui, M. (2002) Mise en place d'un système de suivi et de surveillance de la qualité des eaux souterraines et des sols dans le périmètre irrigué du Tadla au Maroc. In Marlet, S. and Ruelle, P. (éditeurs): Vers une maîtrise des impacts environnementaux de l'irrigation. *Actes de l'atelier du PCSI*, Montpelier, France. 11 pages.

Berkat, O. and Tazi, M. (2004) Country pasture/Forage resource profile. http://www.fao.org/ag/agp/agpc/doc/counprof/morocco/morocco.htm.

Casas, S. (1995) Salinity assessment based on combined use of remote sensing and GIS. Use of remote sensing techniques in irrigation and drainage, (Editor) Smedema, L.K. Expert consultations, Montpellier, France 2-4 Novembre, Water paper 4, FAO, Rome: 185-190

Chapman, J.E., Rothery, D.A., Francis, P.W. and Pontual, A. (1989) Remote sensing of vaporite mineral zonation in salt flats (salars). *International Journal of Remote Sensing*, 10: 245 - 255.

Crowley, J.K. (1991) Visible and near-infrared (0.4-2.5 μm) reflectance spectra of playa evaporite minerals. *Journal of Geophysical Research*, 96(16): 231- 240.

Csillag, F., Pasztor, L. and Biehl, L. (1993) Spectral band selection for the chracterization of salinity statues of soils. *Remote Sensing of the Environment,* Vol. 43: 231-242.

Deschamps, P.Y., Herman, M., and Tanre, E. (1981) Influence de l'atmosphere en télédétection des resources terrestres. Modélisation et possibilités de correction. Signatures spectrales d'objets en télédétection, Avignon, 8-11 Septembre : 543-558.

Dehaan, R.L. and Taylor, G.R. (2002) Field-derived spectra of salinized soils and vegetation as indicators of irrigation-induced soil salinization. *International Journal of Remote Sensing*, 80: 406 - 417.

Drake, N. A. (1995) Reflectance spectra of evaporite minerals (400-2500 nm): applications for remote sensing. *International Journal of Remote Sensing*, 16: 2555 - 2571.

Dwivedi, R.S. and Rao, B.R.M. (1992) The selection of the best possible Landsat TM band combination for delineating salt-affected soils. *International Journal of Remote Sensing*, 13: 2051-2058.

FAO (2005). The state of land, water and plant nutrition resources in Morocco, Land Resources Information Systems in the Near East-99. http://www.fao.org//DOCREP/005/Y4357/y4357e11.htm

Fraser, D. and Joseph, S. (1998) Mapping soil salinity in the Murray Valley (NSW) using satellite imagery. *Proceedings of the 9th Australasian Remote Sensing and Photogrammetry Conference*, Sydney, Australia. Paper published on CD.

Friedman, S. (2005) Soil properties influencing apparent electrical conductivity: a review. Computers and Electronics in Agriculture, Issues 1-3, March: 45-70.

Gardner, G. (1996) Shrinking Fields: Cropland loss in a world of eight billion. Worldwatch paper 131, Worldwatch insititute, Wahington, D.C. 56 pages.

Ghassemi, F., Jakeman, A.J. and Nix, H.A. (1995) Salinisation of land and water resources: human causes, extent, management and case studies. Center for resource and environmental studies, The Australian National University, Canberra, Australia. 125 pages.

Goosens, R., El Badawi, M., Ghabour, T., and De Dapper, M. (1998) A simulated model to monitor the soil salinity in irrigated arable land in arid areas based upon remote sensing and GIS. EARSeL Advances in Remote Sensing, Vol. 2(3): 165-171.

Gupta, R.K. and Abrol, I.P. (1990) Salt-affected soil: Their reclamation and management for crop production. *Advances in Soil Science Volume 11 Soil degradation,* (Editors) Lal, R., Stewart, B.A. Springer-Verlag, New York. 288 pages.

Hammani, A., Kuper, M., Debbarh, A., Bouarfa, S., Badraoui, M. and Bellouti, A. (2004) Evolution de l'exploitation des eaux souterraines dans le périmètre irrigué du Tadla. *Actes du séminaire sur la modernisation de l'agriculture irriguée*, Rabat, Maroc. 8 pages.

Hashem, M., El-Khattib, Nabil, El-Mowelhi, M. and Abd El-Salam, A. (1997) Desertification and land degradation using high resolution satellite data in the Nile Delta, Egypt. *IEEE*: 197-199.

Hick, P.T. and Russel, W.G.R. (1990) Some spectral considerations for remote sensing of soil salinity. *Australian Journal of Soil Research*, 28: 417-431.

Hillel, D. (2000) Salinity management for sustainable irrigation: Integrating science, environment, and economics. World Bank, Washington. 104 pages.

Howari, F.M., Goodell, P.C. and Miyamoto, S. (2002) Spectral Properties of Salt Crusts Formed on Saline soils. *Journal of Environmental Quality,* Vol. 31:1453-1461.

Hunt, G.R., Salisbury, J.W., and Lenhhoff, C.J. (1971) Visible and near infrared spectra of minerals and rocks: III. Oxides and Hydroxides. *Modern Geology*, 2: 193-205.

IDNP (2003) Indo-Dutch Network Project: A Methodology for Identification of Waterlogging and Soil Salinity Conditions Using Remote Sensing. Central Soil Salinity Research Institute, Karnal, India. 78 pages.

Jankowski, J. and Ackworth, R.I. (1999) Personal communication by Dehaan, R.L. et Taylor, G.R. (2002) Field-derives spectra of salinized soils and vegetation as indicators of irrigation-induces soil salinization, *Remote Sensing of Environment* 80: 406-417.

Joshi, D.C., Toth, T. and Sari, D. (2002) Spectral reflectance characteristics of Na-carbonate Irrigated Arid Secondary Sodic Soil. *Arid Land Research and Management* ,Vol. 16: 161-176.

Kaufman, Y.J. and Sendra, C. (1988) Algorithmfro atmospheric corrections, International Journal of Remote Sensing, 9: 1357-1381.

Khan, N.M., Rastoskuev, V.V., Shalina,E.V. and Sato,Y. (2001) Mapping Salt-Affected Soils using remote sensing Indicators – A simple approach with the use of GIS IDRISI. *Proceedings of the 22nd Asian Conference on Remote Sensing*, 5-9 November, Singapore. Center for Remote Imaging, sensing and Processing (CRISP), National University of Singapore; Singapore Institute of Surveyors and Valuers; Asian association on remote sensing. 5 pages.

Menenti M, Bastiaanssen WGM, Hefny K, Abd El, Karim MH. (1991) *Mapping of ground water losses by evaporation in the Western Desert of Egypt.* DLO Winand Staring Centre, Report no. 43, Wageningen, The Netherlands. 116 pages.

Metternicht, G.I. and Zinck, J.A. (2003) Remote sensing of soil salinity: potentials and constraints. *Remote sensing of the environment*, 85: 1 – 20.

Metternicht, G. I. (1998) Fuzzy classification of JERS-1 SAR data: an evaluation of its performance for soil salinity mapping. *Ecological Modelling*, 111: 61 - 74.

Metternicht, G. I. and Zinck, J. A. (1997) Spatial discrimination of salt- and sodium-affected soil surfaces. *International Journal of Remote Sensing*, 18: 2571 - 2586.

Metternicht, G.I. (1996) Detecting and monitoring land degradation features and processes in the Cochamba valleys, Bolivia: A synergistic approach. ITC publication No.36, International Institute for Geo-information Science and Earth Observation. Enschede, The Netherlands. 390 pages.

Mougenot, B. (1993) Effets des sels sur la réflectance et télédétection des sols salés. Cahiers ORSTOM, Série Pédologie, 28 : 45 - 54.

Mougenot, B., Pouget, M. and Epema, G. (1993) Remote sensing of salt affected soils. *Remote sensing review* Vol. 7: 241-259.

Mulders, M. (1987). *Remote sensing in soils science. Development in soil science.* Amsterdam, The Netherlands: Elsevier. 379 pages.

Mulder, M.A. and Epema, G.F. (1986) The thematic mapper : A new tool for soil mapping in arid areas. *ITC Journal* ,Vol. 1: 24-29.

NASA, (2006) Earth Observing 1 (EO-1) User's Guide. http://eo1.usgs.gov/userGuide/index. html.

Norman, C.P., Lyle, C.W., Heuperman, A.F. and Poulton, D. (1989) Tragowel Plains – Challenge of the Plains. In: Tragowel Plains Salinity Management Plan, Soil Salinity Survey, Tragowel Plains Subregional working group. Victorian Department of Agriculture, Melbourne :49-89

ORMVAT (2004) Rapport sur le suivi de la qualité des sols, Octobre – Novembre. ORMVAT, Maroc. 6 pages.

ORMVAT (2009) Exploitation DGRID. Consulté le 28/08/2009. http://ormvatadla.com/site/exploitation-dgrid/

Peverill, K.I., Sparrow, L.A. and Reuter, D.J. (1999) Soil analysis: an interpretation manual. CSIRO Publishing, Australia. 317 pages.

Postel, Sandra (1999) Pillar of Sand: Can the irrigation miracle last. Worlwatch book. Norton and Company, New York. 315 pages.

Price, J.C. (1987) Radiometric Calibration of Satellite Sensors in the Visible and Near Infrared: History and Outlook, *Remote Sensing of Environment*, 22:3-9.

Rao, B., Sankar, T., Dwivedi, R., Thammappa, S., Venkataratnam, L., Sharma, R. and Das, S. (1995) Spectral behaviour of salt-affected soils. *International Journal of Remote Sensing,* 16: 2125 – 2136.

Rao, B.R., Dwivedi, R.S., Venkataratnam, L., Ravishankar, T., Thammappa, S.S., Bhargawa, G.P. et Singh, A.N. (1991) Mapping the magnitude of sodicity in part of the Indo-Gangetic plains of Uttar Pradesh, Northern India using Landsat-TM. *International journal of remote sensing,* Vol. 12: 419-425.

Richards, L.A. (1954) Diagnosis and improvements of saline and alkali soils. U.S. Salinity Laboratory DA, US Department of Agriculture Hbk 60.160 pages.

Richards, J.A. (1993). Remote Sensing Digital Image Analysis: An Introduction. Springer-Verlag, Berlin.

Singh, R.P. and Srivastav, S.K. (1990) Mapping of water-logged and saltaffected soils using microwave radiometers. International Journal of Remote Sensing, 11: 1879-1887.

Smedema, L.K. (1995) Salinity control in irrigated land: Use of remote sensing techniques in irrigation and drainage. *Proceeding of the expert consultation, session 3- Drainage and salinity monitoring and control.* Montpellier, France, 2-4 November, 1993. FAO, Water Reports 4: 141-150.

Stewart, B.A. (2005) Food security and Production in Dryland Regions. *Climate change and Global food security.* (Editors) Lal, R., Uphoff, N., Stewart, B.A. and Hansen, D.O., CRC Press, Taylor and Francis group, Florida: 363-382.

Tanré, D. (1982) Interaction rayonnement-aérosols applications a` la télédétection et au calcul du bilan radiatif, Thèse, Université des Sciences et Techniques de Lille.

Taylor,G. R., Mah, A. H., Kruse, F. A., Kierein-Young, K. S., Hewson, R. D. and Bennett, B. A. (1996) Characterization of saline soils using airborne radar imagery. *Remote Sensing of Environment*, 57: 127 - 142.

Taylor, G.R., Bennett, B.A., Mah, A.H. and Hewson, R.D. (1994) Spectral properties of salinised land and implications for interpretation of 24 channel imaging spectrometry. *Proceedings of the first international remote sensing conference and exhibition,* Strasbourg, France, Vol. 3: 504 - 513.

Taylor, G. and Deehan, R. (2000) Mapping soil salinity with hyperspectral imagery. Proceedings of the 14th international conference applied geologic remote sensing, Veridan ERIM International, 6th November, Las Vegas, Nevada: 512 – 519.

Teillet, P.M. Fedosejevs, G., Ahern, F.J. and Gauthier, R.P. (1994) Sensitivity of Surface Reflectance Retrieval to Uncertainties in Aerosol Optical Properties, *Applied Optics*, 33(18): 3933-3940.

Teillet, P.M. (1992) An Algorithm for the Radiometric and Atmospheric Correction of AVHRR Data in the Solar Reflective Channels, *Remote Sensing of Environment*, 41: 185-195.

Teillet, P.M. and Santer, R.P. (1991) Terrain Elevation and Sensor Altitude Dependence in a Semi-Analytical Atmospheric Code. Canadian Journal of Remote Sensing, Vol. 17, No. 1.

US Salinity Laboratory (1954) Diagnoses and Improvement of Saline and Alkali Soils. Agriculture Handbook No. 60. United States Department of Agriculture, Washington, D.C. 631 pages.

Verma, K.S., Saxena, R.K., Barthwal, A.K. and Deshmukh, S.N. (1994) Remote sensing technique for mapping salt affected soils. *International Journal of Remote Sensing,* Vol. 15(9): 1901-1914.

Vidal, A., Maure, H., Durand, H. and Strosser, P. (1996) Remote sensign applied to irrigation system management : Example of Pakistan. *EURISY ColloquiumL Satellite Observation for Sustainable Development in the Mediterranean Area*: 132-142.

Vincent, B, Frejefond, E., Vidal, A. and Baqri, A. (1995) Drainage performance assessment using remote sensing in the Gharb Plain, Morrocco. *Use of remote sensing techniques in irrigation and drainage*, (editors) Vidal, A. et Sagardoy, J.A., Water report 4, FAO, Rome: 155-164.

Zinck, J.A. (2000) Monitoring soil salinity from remote sensing data. From the 1st workshop EARSel Special Interest Group on Remote Sensing for Developing Countries: 359-368.

Zuluaga, J.M. (1990) Remote Sensing applications in irrigated management in Mendoza, Argentina. Remote sensing in evaluation and management of irrigation, (editor) Menenti, M., Instituto Nacional de Ciencia y Técnicas Hidricas, Mendoza, Argentina: 37-58.